REMARKS

The Examiner's attention to the present application is noted with appreciation. The Examiner rejected claims 1-2 under 35 U.S.C. 112, first paragraph, as failing to comply with the enabling requirement. Such rejection is respectfully traversed. The Examiner asks, "It is not clear if the secondary coherent light emission is the coherent laser light *intended to be generated* by the apparatus, using the hologram, then where does this coherent laser light come from to record the hologram at first place?" The present invention uses a self-organizing (i.e. automatically formed) *temporary* hologram to create coherence in the primary emission, a technique commonly known as "double phase conjugation". Submitted herewith are three articles (Sternklar et al., Iida et al., and MacCormack et al.) that disclose the use this technique for locking of diode lasers. Also see Horuichi et al. (submitted herewith): "Two input beams exchange their wave front through the MPPC, and the diffracted beam from the master laser becomes the phase conjugate wave of the direct output from the slave laser. Thus, the beam from the master laser propagates toward the slave laser and is coupled to the active medium automatically in accordance with the property of the phase conjugate wave." Petris et al. provide a general statement of the state of the art of adaptive coupling using phase conjugation in the Introduction to the paper. Thus this technique is quite well known in the established literature, and the use of it in conjunction with the method disclosed in the present invention would be obvious to one skilled in the art. Further, the enclosed references discuss phase locking of the diodes, addressing the related concern of the Examiner similarly.

The Examiner rejected claims 1 and 2 under 35 U.S.C. § 103(a) as being unpatentable over Roess in view of Ritter et al. Such rejection is respectfully traversed, particularly as to the claims as amended. Neither of the references cited uses a photorefractive crystal or photorefractive phase conjugation. Thus the cited references do not teach all of the claim limitations, which is required per MPEP 2143.03.

The Examiner rejected claims 3 and 4 under 35 U.S.C. § 103(a) over Roess in view of Psaltis et al. Applicant assumes that the Examiner will so reject claims 1 and 2, further in view of Ritter et al., as amended. Such rejections are respectfully traversed. Roess creates a hologram by "superimposing *a*

spherical wave with a series of spherical waves from the various single resonators of the partial oscillators..." (col. 2, lines 49-51, emphasis added). However, as is well known in the art (and described in the present application on page 4, lines 24-26), a photorefractive crystal would superimpose a plurality of *phase conjugates of the spherical waves*, NOT a single "spherical wave", with the series of spherical waves. Thus, combining the photorefractive crystal of Psaltis et al. with the apparatus of Roess would change the latter's principle of operation, thereby rendering the combination of references improper under MPEP 2143.01.

In view of the above amendments and remarks, it is respectfully submitted that all grounds of rejection and objection have been avoided and/or traversed. It is believed that the case is now in condition for allowance and same is respectfully requested.

If any issues remain, or if the Examiner believes that prosecution of this application might be expedited by discussion of the issues, the Examiner is cordially invited to telephone the undersigned agent for Applicant at the telephone number listed below.

Also being filed herewith is a Petition for Extension of Time to April 21, 2005, together with the appropriate fee. Authorization is given to charge payment of any additional fees required, or credit any overpayment, to Deposit Acct. 13-4213. A duplicate of the Petition paper is enclosed for accounting purposes.

Respectfully submitted,

By: 

Philip D. Askenazy, Reg. No. 56,721
Direct line: (505) 998-6132

PEACOCK, MYERS & ADAMS, P.C.
Attorneys for Applicant(s)
P.O. Box 26927
Albuquerque, New Mexico 87125-6927

Telephone: (505) 998-1500

Facsimile: (505) 243-2542

Customer No. 005179

G:\AMDS\Los&Stig\Offerhaus - RCE amendment.doc

Beam coupling and locking of lasers using photorefractive four-wave mixing

Shmuel Sternklar, Shimon Weiss, Mordechai Segev, and Baruch Fischer

Department of Electrical Engineering, Technion, Haifa 32000, Israel

Received April 11, 1986; accepted May 30, 1986

We discuss the use of photorefractive four-wave mixing for coupling and locking of lasers. A demonstration of the double phase-conjugate mirror and the semilinear passive phase-conjugate mirror, pumped simultaneously by different lasers, is described. Cleanup of a distorted laser beam using another local laser and configurations for the phase locking of lasers are discussed.

We present various four-wave mixing (4WM) configurations[1] for coherent beam combining, amplification, and cleanup as well as laser locking using photorefractive crystals. In these devices, as opposed to two-wave mixing schemes,[2] light feedback into the different lasers that are mutually pumping the 4WM process can cause beam combining and laser locking. Two 4WM configurations[1,3] were studied, the double phase-conjugate mirror (DPCM) and the semilinear passive phase-conjugate mirror (PPCM), shown schematically in Fig. 1.

We start with the operation of the DPCM using two separate lasers as inputs to the opposite sides of a $BaTiO_3$ crystal, as shown in Figs. 1(a) and 2. Laser 1 was a Spectra-Physics Model 165 argon-ion laser operating at its 488-nm line in multimode operation. It was situated in a different room from the crystal and from laser 2, at an optical path length greater than 10 m from the crystal. Beam 4 from this laser entered the $z = 0$ face of the crystal. Laser 2 was a Spectra-Physics Model 171 argon-ion laser, also operating in multimode at its 488-nm line. Beam 2 from this laser, which was situated on the same table as the crystal, entered the $z = l$ face of the same crystal after having traversed 1 m from the laser. The angles of the input beams, which were extraordinarily polarized, were similar to the semilinear PPCM configuration.[1] The two input beams were loosely focused by lenses 1 and 2, with a focal length of 15 cm, and overlapped in the crystal. We observed that these two independent inputs coupled into each other by mutually pumping a single, efficient 4WM process, resulting in the emergence of phase-conjugate output beams $A_1 \propto A^*_2$ and $A_3 \propto A^*_4$, where A_i are the complex amplitudes of the beams. We stress that, in this configuration, beam A_4 supplies the photons for beam A_1 and beam A_2 is the source of photons for beam A_3, so the two input beams are self-bent into each other. Care was taken to ensure that no internal-reflection mechanism nor a two-wave mixing process could form the phase conjugation. In this configuration, each of the input beams 2 and 4 forms its own writing mates 1 and 3, respectively. Thus, the beams have a minimal coherence requirement. In a former paper,[3] we analyzed and demonstrated the DPCM. Its transmission or self-bending efficiency $[A_1(l)/A_4(0) = A_3(0)/A_2(l)]$ approaches unity for high coupling efficiency and negligible absorption. This can lead to high reflection amplification $[A_1(l)/A_2(l)$ or $A_3(0)/A_4(0)]$.

The self-induced gratings and the passive buildup of the two output beams in the DPCM pumped with incoherent, separate lasers are possible even without an exact frequency matching of the pumps. The restriction on the maximum allowable difference in wavelengths $\Delta\lambda$ is dictated by the volume gratings' selectivity, $(\Delta\lambda/\lambda) \lesssim (\Lambda_g/l)f$, where Λ_g is the grating period, l is the interaction width in the crystal, and f is a geometric factor for the 4WM configuration.[4] Typical values of $l \sim 1$ mm and $\Lambda_g \sim 2$ μm give $\Delta\lambda \lesssim 1$ nm. We emphasize that the gratings' limited frequency response, which is of the order of 1 Hz for $BaTiO_3$, does not impose restrictions. Thus different frequencies of

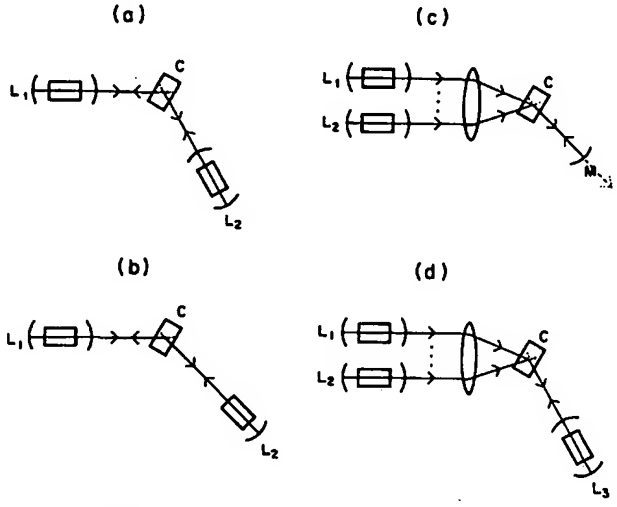

Fig. 1. 4WM schemes in a photorefractive crystal C for laser coupling: (a) the DPCM with two lasers, L_1 and L_2; (b) laser locking with coupled cavities using the DPCM; (c) semilinear PPCM with multiple inputs; (d) proposed multiple laser locking using the DPCM.

0146-9592/86/080528-03$2.00/00

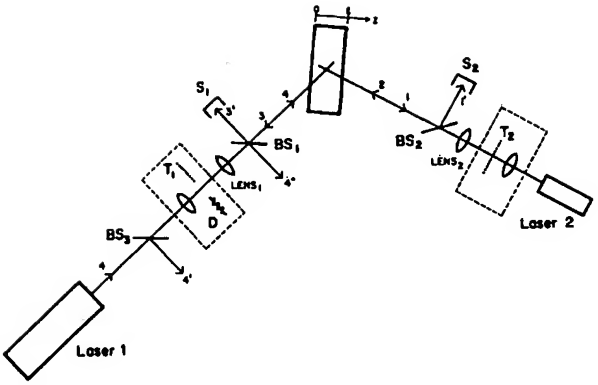

Fig. 2. Schematic of the two-laser-pumped DPCM. The boxed components were for the image-conjugation (including optics for beam expansion) or beam-cleanup experiments. BS's, beam splitter; D, distortion; LENS's, lenses used for focusing input beams 4 and 2 in the crystal, both with a focal length of 15 cm; S's, screens; T's, transparencies.

the same line of the argon-ion lasers for the two pumps are permissible.

The image-conjugating ability of this DPCM was tested by using two transparencies, as shown in Fig. 2. Slides T_1 and T_2 were simultaneously illuminated by expanded beams 4 and 2, respectively, which were then loosely focused in the crystal. The crystal was situated near the focal plane of lenses $LENS_1$ and $LENS_2$. The exact position of the slides between the beam-expanding optics and focusing lenses $LENS_1$ and $LENS_2$ was found to be insignificant. Portions of the phase-conjugate output beams 3′ and 1′ as seen simultaneously on screens S_1 and S_2, respectively, are shown in Figs. 3(a) and 3(b). High-quality images, as for the previously reported DPCM with one common laser input,[3] were obtained. As in previous work with the DPCM[3] and image-bearing photorefractive oscillators,[3,5] no intensity cross talk was observed. In the ring PPCM,[1] the oscillation also produces phase-conjugate counterpropagating beams, resulting in the maximum spatial overlap and gain in the photorefractive crystal.

Spatial phase aberrations in a laser beam can be cleaned up by using the undistorted beam from another local laser source. We investigated this capability by removing T_1 and T_2 and inserting a clear transparency smeared with Vaseline (D), which severely distorted input beam 4. The amount of distortion was checked by sampling beam 4 before the distortion (beam 4′) and interferring it with a portion of the aberrated input 4″, as shown in Fig. 3(c). An undistorted input beam 2 from laser 2 interacted with beam 4 in the crystal, so that a clean phase-conjugate output beam 1 emerged. An interferometric check of 1′ with 4′ revealed virtually aberration-free wave fronts, as shown in Fig. 3(d). This system, as opposed to another two-wave mixing device,[2] does not require coherent beams at the input.

We also studied the beam-combining capability of the multipumped semilinear PPCM shown in Fig. 1(c). Here a single oscillation between the crystal and the mirror M may build up owing to pumping with an array of lasers. This can result in beam combining in the common oscillating beam as well as phase locking of the laser array owing to phase-conjugate feedback of the 4WM process. An experimental evaluation of this scheme was carried out by using the two argon-ion lasers with beam intensities of 15 mW. Oscillation intensity in the crystal-mirror cavity (with mirror reflectivity of 0.7) due to the simultaneous pumping of the lasers typically exceeded by a factor of 3 the sum of the individual oscillation intensities for each laser operating separately. We noticed that even in cases when laser 2 was unable to build up a 4WM oscillation alone, laser 1 induced a coupled oscillation fed by both lasers, so that the phase conjugate of both lasers' beams still emerged. A detailed analysis of this system including the mutual interaction of the pumps is under way. Another configuration that could be used for beam combining is the multipumped unidirectional ring oscillator.[1]

In these 4WM configurations, the beam-coupling mechanism adapts to inputs from different lasers and acts as a dynamic self-adjusted grating to channel energy from each laser into the other. This suggests its use for coherently combining and phase locking lasers,[6] as shown in Fig. 1. Phase locking of the two argon-ion lasers initially operating in multimode (without étalons) was studied in the DPCM scheme of Fig. 1(b). The output mirrors were removed from both lasers and replaced by a single variable beam splitter set at an intensity transmission of about 0.2 at the output of the laser 1 cavity. Here the cavities are

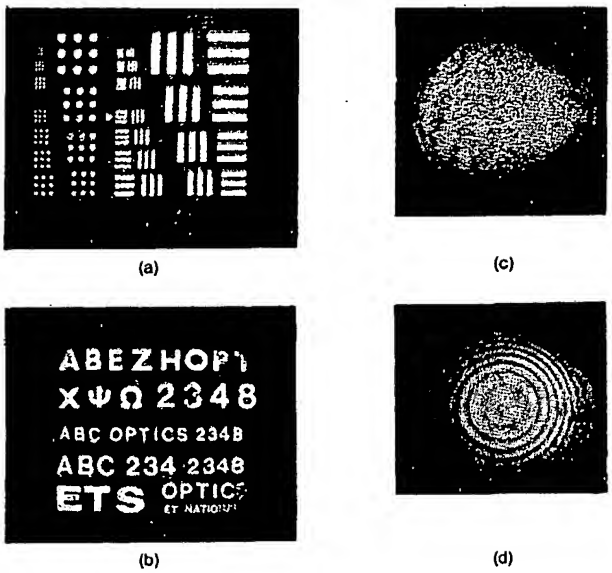

Fig. 3. Results of the phase-conjugation [(a), (b)] and beam-cleanup [(c), (d)] experiments with the two-laser-pumped DPCM of Fig. 2. (a) Phase-conjugate output of T_1 seen at S_1 and simultaneously; (b) phase-conjugate output of T_2 seen at S_2; (c) interferometric check of the input beam 4 distortion after passing through distorter D; (d) interferometric check of the undistorted phase fronts of output beam 1 due to beam cleanup by the DPCM.

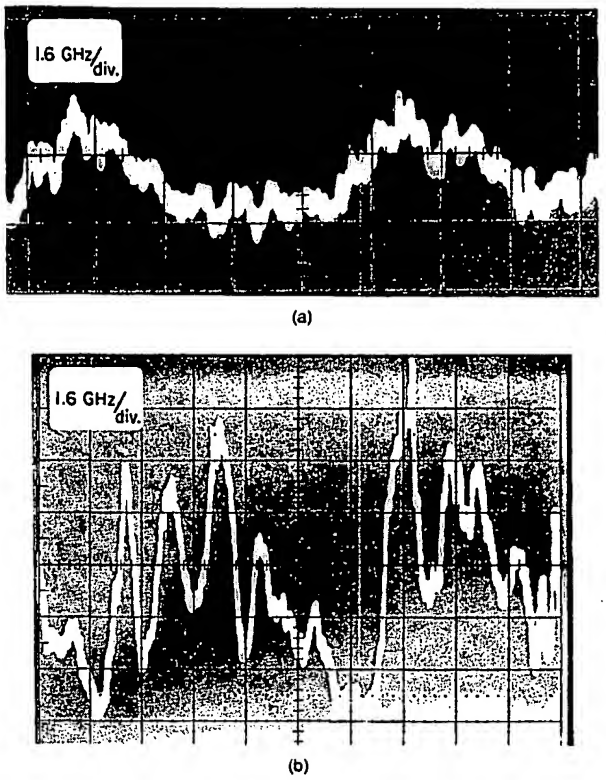

Fig. 4. (a) Two successive scans of the laser L_2 spectrum [in Fig. 1(b)] with cavity-length detuning, measured with an 8-GHz free-spectral-range étalon at a scan rate of 500 Hz. (b) Spectra after cavity tuning displaying short-term phase locking. Note the change in the spectra for the two scans, as discussed in the text.

coupled to each other, permitting frequency selectivity for proper cavity lengths. Phase locking is possible for small-cavity detuning and depends on the energy coupling between the cavities.[7,8] We set up two cavities with lengths of approximately 1.3 and 13 m with an adjustable arm length of the longer laser 2 cavity using a sliding corner cube. The spectrum of laser 2 before tuning, measured with an 8-GHz free-spectral-range étalon at a scan rate of 500 Hz, is shown in Fig. 4(a). This spectrum was identical to that of laser 2 looking into free space. We observed that, with simple matching of the cavity lengths, without a change in the other parameters, the lasers oscillated in a few common modes owing to the frequency selectivity of the coupled cavities. The resulting spectrum, seen in Fig. 4(b), was observed to be stable for periods of the order of 1 msec. We emphasize that the lasers were neither externally stabilized nor isolated. Long-term locking is expected with stabilized lasers and shorter cavity lengths. Diode-laser locking should also prove to be simpler, given these lasers' easier line selection and control by way of the diode current and higher light coupling.[9] This will permit locking of laser arrays, as shown schematically in Figs. 1(c) and 1(d). We are currently investigating these topics.

We have demonstrated the operation of the DPCM and the semilinear PPCM pumped simultaneously by two different argon-ion lasers. Owing to the 4WM process, the pumping beams couple energy into each other and can cause beam combining and laser locking. We have demonstrated beam cleanup with the DPCM and beam combining with the semilinear PPCM. In addition, we have presented results showing short-term phase locking of the two argon ion lasers using the DPCM and have discussed configurations for the locking of laser arrays.

This research was partially supported by the Technion VPR fund.

References

1. M. Cronin-Golomb, B. Fischer, J. O. White, and A. Yariv, J. Quantum Electron. **QE-20**, 12 (1984); J. O. White, M. Cronin-Golomb, B. Fischer, and A. Yariv, Appl. Phys. Lett. **40**, 450 (1982).
2. A. E. T. Chiou and P. Yeh, Opt. Lett. **10**, 621 (1985).
3. S. Weiss, S. Sternklar, and B. Fischer (submitted to Opt. Lett.).
4. H. Kogelnik, Bell Syst. Tech. J. **48**, 2909 (1969).
5. B. Fischer, S. Sternklar, and S. Weiss, Appl. Phys. Lett. **48**, 1567 (1986).
6. H. L. Stover and W. H. Steier, Appl. Phys. Lett. **8**, 91 (1966); C. L. Tang and H. Stats, J. Appl. Phys. **38**, 323 (1967).
7. M. B. Spencer and W. E. Lamb, Phys. Rev. A **5**, 893 (1972).
8. M. J. Adams and J. Buns, IEEE J. Quantum Electron. **QE-20**, 99 (1984); H. K. Choi, K. L. Chen, and S. Wang, IEEE J. Quantum Electron. **QE-20**, 385 (1984).
9. G. R. Hadley, IEEE J. Quantum Electron. **QE-22**, 419 (1986), and references cited therein.

ELSEVIER

1 May 2002

Optics Communications 205 (2002) 437–448

OPTICS COMMUNICATIONS

www.elsevier.com/locate/optcom

Adaptive self-aligning, bi-directional interconnection using double phase conjugation in Rh:$BaTiO_3$

A. Petris[b], M.J. Damzen[a,*], V.I. Vlad[b]

[a] *The Blackett Laboratory, Imperial College of Science, Technology and Medicine, Prince Consort Road, London SW7 2BW, UK*
[b] *Department of Lasers, The Institute of Atomic Physics, National Institute of Laser, Plasma and Radiation Physics, R-76900 Bucharest, Romania*

Received 20 November 2001; accepted 5 March 2002

Abstract

The results of an experimental demonstration of a very efficient adaptive interconnection between two low power lasers, using a double phase-conjugate mirror (DPCM) in Rh:$BaTiO_3$ are presented. Using low power incident beams, high phase conjugate reflectivity (~120%) and, simultaneously, high coupling transmission efficiency (~50%) of the double phase conjugation process have been measured. After subtracting the losses in the crystal, this diffraction efficiency corresponds to an almost complete deflection of one input laser beam into the direction of the other one. We compare our experimental results on phase conjugate reflectivity and coupling transmission efficiency with analytical predictions of DPCM and find they are in agreement. The build-up time of the interconnection channel was measured taking into account the competition of DPCM with self-pumped phase conjugation. The robustness of the interconnection to out-of-plane angular changes of the direction of one of the input beams is demonstrated. The influence of the laser beam modulation on the interconnection efficiency is studied. We show that the interconnection efficiency is very good even at very strong modulation of the input beams.

PACS: 42.65.Hw; 42.70.Nq

Keywords: Adaptive optics; Optical interconnections; Photorefractive crystals; Double phase conjugate mirror; Rh:$BaTiO_3$

1. Introduction

The coupling of two or more incoherent laser beams is important for optical communications, optical interconnects, multi-beam coupling into an optical fiber, etc. In these applications, it is necessary to establish a link between an optical source (the input) and an optical receiver (the output). The input can be a single laser beam (a point source), or a 1D or 2D array of laser beams (lasers, optical fibers). The receiver can be a single detector (fiber) or an array of detectors (fibers). In a bi-directional link, each terminal element of the link includes a source and a receiver.

Photorefractive materials, which can provide an efficient interaction of light beams even for

* Corresponding author. Fax: +44-20-7594-7744.
E-mail address: m.damzen@ic.ac.uk (M.J. Damzen).

0030-4018/02/$ - see front matter
PII: S0030-4018(02)01367-6

very low intensities, have great potential in adaptive laser beam coupling and interconnections [1–3]. One of the most important nonlinear processes in photorefractive optics is the Mutually Pumped Phase-Conjugation (MPPC). Several configurations of MPPC have been demonstrated and investigated: Bird-wing, Bridge, British I and II, Double-Phase-Conjugate Mirror (DPCM), and others [4–11]. Experimentally it has been observed that the mutual coherence of the two pump beams changes the performance of a mutually pumped phase conjugator considerably [12–14]. The DPCM configuration is the best one when coupling mutually incoherent input beams: the operation of a DPCM conjugator is optimum when using mutually incoherent input beams [12–14].

The phase conjugation provided by a DPCM conjugator is an all-optical solution to the problem of bi-directional adaptive interconnection of two independent laser sources, ensuring the finding of each source by the other one and their reciprocal tracking (Fig. 1(a)). In a DPCM conjugator, the beam conjugated to each pump beam is generated by the other pump beam, and not by each source itself. This fact is essential for finding and tracking of one source by the other one in a bi-directional link. Another advantage is that the DPCM will reconfigure itself if there are small direction changes of incident beams, within some specified angular ranges in the crystal, thus yielding an adaptive tracking and very robust link (Fig. 1(b)).

Among photorefractive materials, the rhodium-doped barium titanate crystal ($Rh:BaTiO_3$) is one of the most interesting due to its large electro-optic coefficient (giving big changes in the refractive index) and good sensitivity in the red and near-infrared (600–1000 nm) [15,16] where are many promising applications of phase conjugate mirrors based on laser diode sources.

In this paper, we present the results of an experimental study on adaptive, self-aligning, bi-directional interconnection (link) of two lasers using DPCM in $Rh:BaTiO_3$. Using low power incident beams, high phase conjugate reflectivity and, simultaneously, high coupling transmission efficiency of the DPCM have been measured. This diffraction efficiency (after subtracting the losses due to Fresnel reflections and absorption in the crystal) corresponds to an almost complete deflection of one input laser beam into the direction of the other one, indicating a very strong coupling between the two lasers. The experimental results on phase conjugate reflectivity and coupling transmission efficiency are compared with the analytical predictions of a simple theoretical model of DPCM. The build-up time of the DPCM coupling channel and the competition with self-pumped phase conjugation (SPPC) are considered and discussed. The change of the coupling efficiency when the input beams become non-coplanar (as in the case when arrays of laser sources are coupled), was studied.

The possibility of transmission of information between the two lasers was demonstrated. The strength of the coupling remains very good even when using a very strong modulation of the input beams.

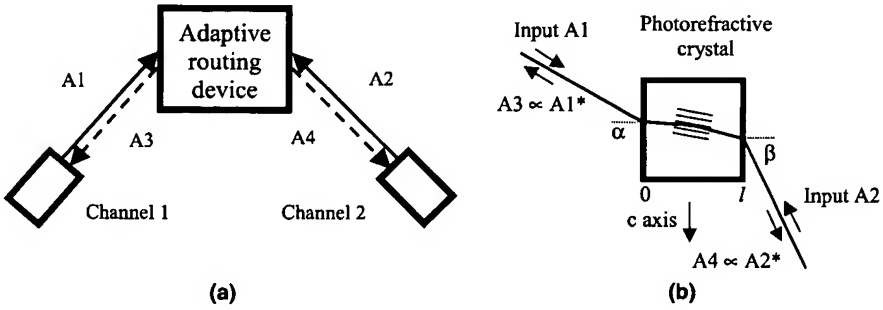

Fig. 1. (a) Bi-directional adaptive routing device; (b) adaptive coupling using DPCM configuration in a photorefractive crystal.

2. Efficient adaptive coupling of two lasers in Rh:$BaTiO_3$ by DPCM

In the studied DPCM configuration (Fig. 1(b)), the beams A1 and A2, from two separate lasers of the same frequency are incident on the opposite faces of the photorefractive crystal. The orientation of the c-axis of the crystal is shown in Fig. 1. Because the input beams are mutually incoherent, they cannot directly couple with each other in the crystal. Light randomly scattered (fanned) from beam A1, travelling across beam A1, coherently couples with this beam and writes a multitude of different refractive index gratings in the photorefractive crystal. A similar process occurs with beam A2: light fanned from this beam coherently couples with beam A2 and writes another set of beam-fanning gratings. Each input beam tends to erase most of the beam-fanning gratings produced by another one.

However, A2 is incident at the Bragg angle for a small set of beam-fanning gratings produced by A1. The diffracted beam A3, which is the phase conjugate replica of the beam A1, efficiently couples with beam A2 (they are mutually coherent). The result of a similar process with the beam A1 is the beam A4, the phase conjugate replica of the beam A2. Since the gratings written by the pairs of beams A3, A2 and A4, A1, respectively, have an optimal overlapping, the conjugated beams A3, A4 grow in strength, reinforcing their shared grating. The other beam-fanning gratings are washed out. In this way, diffraction from the common grating is responsible for the generation of A3 and A4, phase conjugate beams of the mutually incoherent input beams, A1 and A2, respectively.

The overall efficiency of the DPCM configuration is evaluated using two parameters: the phase conjugate reflectivity, R^*, for the two input beams and the coupling transmission efficiency, T, for these beams. With the notations used in Fig. 1(b) for the beams, these parameters are defined as ratios of corresponding beam powers:

$$R_1^* = \frac{P_{A3}(0)}{P_{A1}(0)}, \quad R_2^* = \frac{P_{A4}(l)}{P_{A2}(l)}, \tag{1}$$

$$T_1 = \frac{P_{A4}(l)}{P_{A1}(0)}, \quad T_2 = \frac{P_{A3}(0)}{P_{A2}(l)}. \tag{2}$$

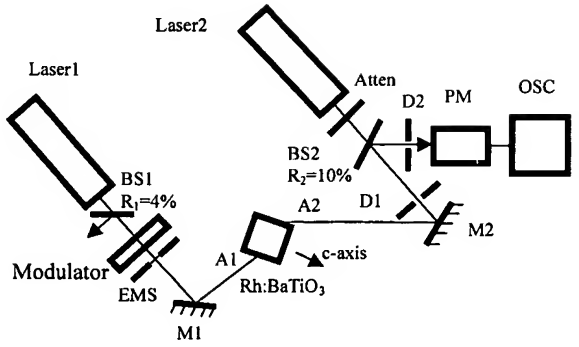

Fig. 2. The experimental setup for coupling of two lasers by DPCM in Rh:$BaTiO_3$.

The experimental arrangement set-up to study the interconnection of two He–Ne lasers by DPCM in Rh:$BaTiO_3$ is shown in Fig. 2.

Two separate He–Ne lasers were used as mutually incoherent light sources (A1 and A2). The input beams, A1 and A2, are extraordinary polarised, in order to access the maximum electro-optic coefficient of the crystal. The power of the input beams are: $P_{A1} = 2.55$ mW; $P_{A2} = 1.35$ mW and their diameter is 1.2 mm (at $1/e^2$ from the maximum power value). A fraction of the beams A3 and A4, conjugated to the input beams A1 and A2, respectively, is extracted with the beam splitters BS1 and BS2 with 4% and 10% reflectivity, respectively. For measuring and monitoring the temporal evolution of the conjugate beams, a power-meter (PM) and an oscilloscope (OSC) were used. Two apertures (D1 and D2), with a diameter equal to that of the incident laser beam A2, were placed in the path of the input beam and in front of the detector, respectively, in order to measure only the conjugated beam and to block the contribution of any other diffracted components and of stray scattered light. An electro-mechanical shutter (EMS) was used to switch on or off the beam A1 at preset moments, in DPCM studies.

The Rh:$BaTiO_3$ crystal used in this work has the dimensions $5 \times 5 \times 5$ mm^3 and 400 ppm Rh doping concentration. All faces of the crystal are polished. We measured its small signal absorption coefficient, with a low intensity e-polarised probe beam, obtaining $\alpha_0 = 1.4$ cm^{-1}. The light-induced

transparency of the crystal, was not measured in this crystal, but data for crystals with comparable doping concentration were available.

The angles of incidence of the two input beams were $\alpha = 30°30'$ for the beam A1 and $\beta = 60°30'$ for the beam A2, ensuring a crossing angle of the beams, inside the crystal, of 171°. We adjusted the incidence points of the input beams on the crystal faces to optimise the DPCM.

2.1. The phase conjugate reflectivity and the coupling transmission efficiency

We have measured the power of the beam A4, the phase conjugate of the weaker beam, A2. In the experiment, we also observed a weak diffraction cone (orders of magnitude lower than A4) [13,17–19], in which A4 was well separated and filtered by the apertures D1 and D2.

In Fig. 3, the time evolution of the conjugated beam (A4) power for different input beam (A2) powers is shown. In all these records, at time $t = 0$, the beam A2 was unblocked; at time $t = 100$ s the beam A1 is switched on and the growth of the coupling channel can occur. A delay between the moment when both beam are present in the crystal and the start of coupling channel growth occurs due to the necessary fanning development, which leads to the creation of the shared grating. In Fig. 3, one can observe that the coupling channel more rapidly starts to grow at higher powers of the beam A2.

We have measured the phase conjugate reflectivity $R_2^* = P_{A4}/P_{A2}$ for the weaker input beam A2, and the coupling transmission efficiency of the DPCM device, $T_1 = P_{A4}/P_{A1}$, for the stronger beam A1. The results of R_2^* and T_1 as functions of A2 beam power are shown in Figs. 4(a) and (b). The second parameter is very important for an interconnection, since it measures the efficiency of signal transfer between one light source channel to the other.

From Fig. 4, one can remark that the maximum coupling transmission efficiency reaches ~50% at

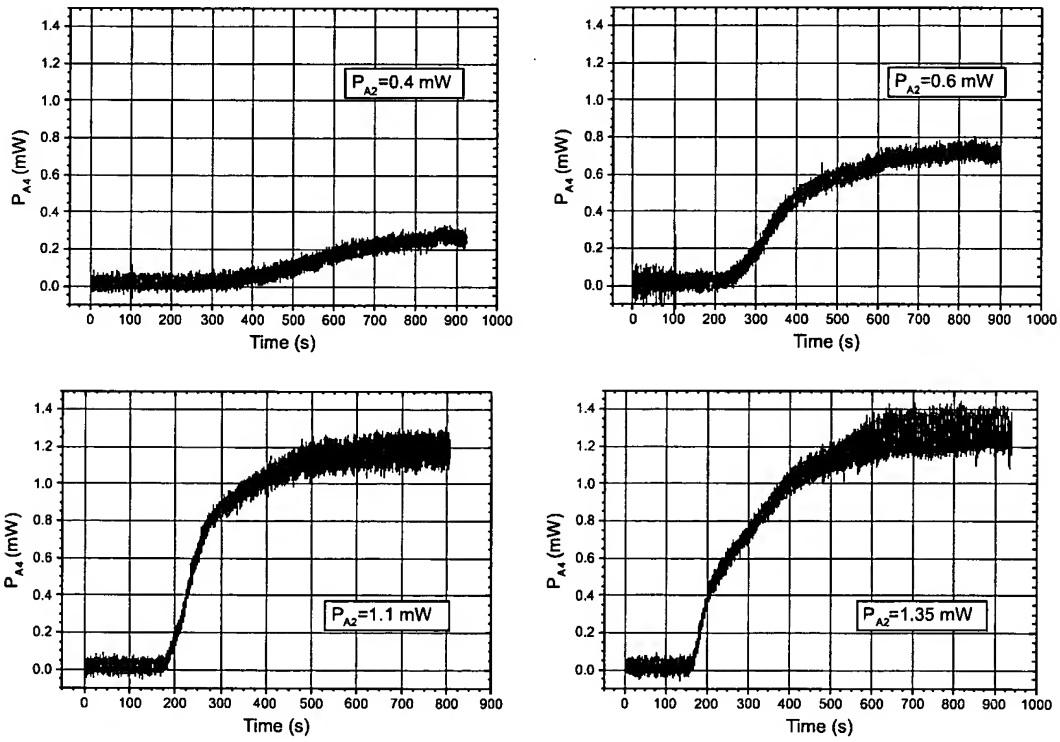

Fig. 3. The time evolution of the conjugated beam (A4) power.

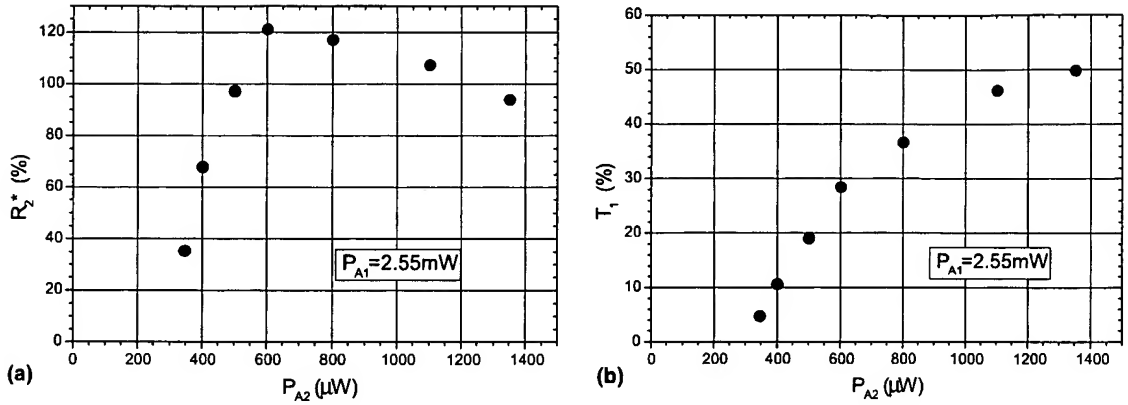

Fig. 4. The efficiency of the DPCM device: (a) the phase conjugate reflectivity, $R_2^* = P_{A4}/P_{A2}$; (b) the coupling transmission efficiency, $T_1 = P_{A4}/P_{A1}$.

maximum power of A2 (ratio of the input beams = 1.9), where the corresponding phase conjugate reflectivity is 95%. The maximum phase conjugate reflectivity obtained in this experiment is 121% (for a ratio of the input beams of 4.25), where the corresponding coupling transmission efficiency takes the value of 29%. Thus, in this DPCM interconnection, the maxima of phase conjugate reflectivity and the coupling transmission efficiency are clearly not obtained for the same input beam ratio.

In comparison with other experiments for coupling of incoherent laser beams by phase conjugation in Rh:$BaTiO_3$ crystals, using a similar configuration [15] or the bird-wing configuration [20], the coupling transmission efficiency and phase conjugate reflectivity obtained by us are better for a bi-directional link. In [20], the coupling transmission efficiency is 6%, a typical value expected for this configuration. In [15] was reported 26% maximum coupling transmission efficiency with 80% reflectivity in DPCM at 800 nm, using a Rh:$BaTiO_3$ crystal with the absorption coefficient for this wavelength, $\alpha = 1.4\ cm^{-1}$ (similar to our crystal absorption at 633 nm). The maximum reflectivity was in that experiment 205%, but associated to very low coupling transmission efficiency, for a ratio of the input beam powers of 50 (at 736 nm; $\alpha = 2.4\ cm^{-1}$).

In order to use this efficient laser coupling in a bi-directional link, we have checked the possible presence of 2 k gratings (induced by each incident beam with its own back-scattered light). In our experimental set-up, we have no optical isolators in the beam paths, so the diffracted components, when the interconnecting DPCM occurs, will feed back to the laser sources and return to the photorefractive crystal. They could create 2 k gratings, if the difference in the optical paths of the direct and back-reflected beams are shorter than the coherence length of the laser. For the interconnection, this leads to a cross-talk (in which signal 1 contains a component of signal 2 and vice versa), which affects negatively its performances [12,14].

In our experimental setup, we have observed the decay of the phase conjugated beam power, when blocking the input beam A2, after the shared grating reached the steady-state. In this case, the conjugated beam, A4, is produced by the beam A1 only. The results from Fig. 5 show clearly that no instantaneous decay in the power of the A4 beam is present. The decay of the conjugated beam A4 is a direct consequence of the erasing action of the beam A1 on the shared grating. If the 2 k grating were present, we would expect to see an instantaneous decay of A4 beam power, when blocking A2. Since this is not seen, we can conclude that 2 k gratings are not important in our experimental coupling and the conjugate of each input beam is produced by the other input beam only.

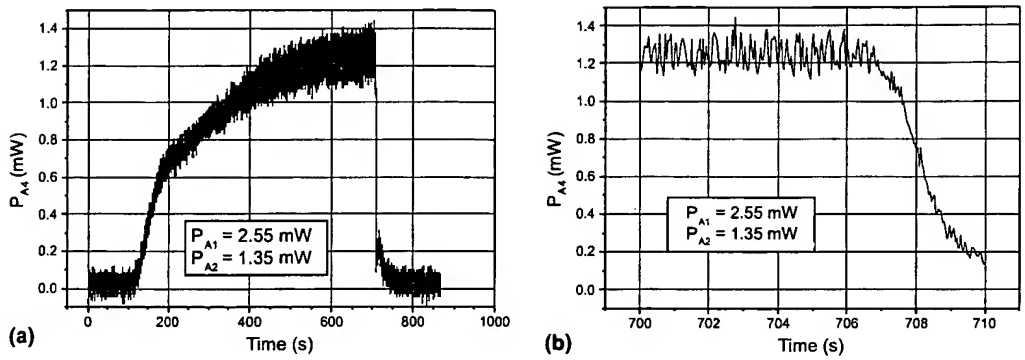

Fig. 5. (a) The rising up of the conjugated beam (A4) power and its decay when the input beam A2 is blocked; (b) the decay of the conjugated beam, immediately after blocking the beam A2, at a different time scale.

2.2. Comparison of experimental results with the theoretical predictions of a simple DPCM model

In order to have an evaluation of the coupling efficiency of the link between the lasers, provided by the DPCM in Rh:$BaTiO_3$, when only the shared transmission grating is present, we have used the results of a simple theoretical model of DPCM without absorption. In this case, the phase conjugate reflectivity and the coupling transmission efficiency were calculated [7], by solving analytically the coupled wave equations that describe the spatial evolution of the input and conjugated beams amplitude.

Neglecting the absorption of the crystal, the phase conjugate reflectivity and the coupling transmission efficiency are dependent on the photorefractive coupling strength, γl, which is the product of the photorefractive coupling coefficient, γ, and the interaction length l, and on the ratio of the input beam powers, $q = P_{A1}/P_{A2}$ (for equal cw laser beam widths). In Rh:$BaTiO_3$ crystal, with no external electric field, the coupling constant is real:

$$\gamma = \frac{2\pi n_1}{\lambda \cos\theta}, \tag{3}$$

where λ is the wavelength of the incident light, n_1 is the amplitude of the refractive index modulation produced by the photorefractive effect and 2θ is the angle between the coupling beams inside the crystal.

Weiss et al. [7], found that the coupling transmission efficiency is symmetric and is given by

$$T_1 = T_2 = T = \left(\frac{1}{4}\right)\left[a^2\left(q^{-(1/2)} + q^{1/2}\right) - \left(q^{-(1/2)} + q^{1/2}\right)^2\right], \tag{4}$$

where the parameter a is related to the coupling coefficient, γ, by the transcendental equation

$$\tanh\left(\frac{\gamma l}{4}a\right) = a. \tag{5}$$

The phase conjugate reflectivities of the DPCM process, for the two incident beams, are [7]

$$R_1^* = T/q \tag{6}$$

and

$$R_2^* = Tq. \tag{7}$$

The operation range of the DPCM configuration is set by the following limits of q:

$$\left(\frac{1+a}{1-a}\right)^{-1} < q < \frac{1+a}{1-a}. \tag{8}$$

We have solved graphically the transcendental equation (Eq. (5)), and we have obtained the parameter a for different coupling strengths, γl. Fig. 6 shows plots of the coupling transmission efficiency (Eq. (4)) and the phase conjugation reflectivity (Eq. (7)) versus the power ratio of the two incident input beams, q, together with the experimental results.

By comparing the theory with the experiment, an evaluation of the coupling strength, γl, of our

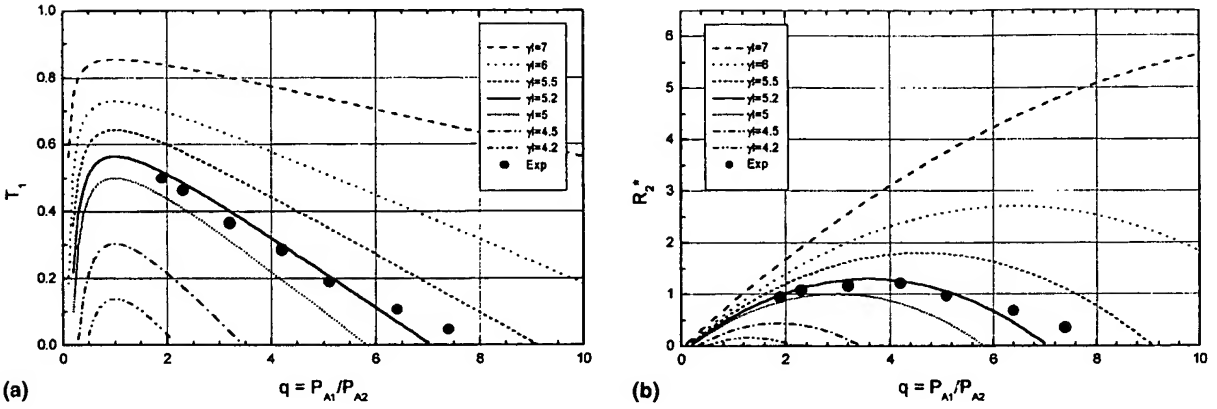

Fig. 6. The coupling transmission efficiency of the phase conjugation process, T_1 (a) and the phase conjugate reflectivity, R_2^* (b), versus the power ratio of the two incident input beams. Theoretical predictions: dashed and dotted lines; experimental results: dots. The coupling strength of our crystal in the DPCM configuration corresponds most closely to $\gamma l = 5.2$.

crystal in the DPCM configuration can be found as $\gamma l = 5.2$ (by a best fit).

The theoretical curves reveal that the maximum values for the coupling transmission efficiency and reflectivity cannot be reached simultaneously and provide the range of the input intensity ratio, q for DPCM operation, for a given coupling strength, γl. For $\gamma l = 5.2$, the maximum coupling transmission efficiency predicted by theory is $\sim$55% for $q \sim 1$. The experimental values of coupling transmission efficiency were limited by the available laser power (P_{A2}) at a maximum of $\sim$50% for $q = 1.9$ (Fig. 4(b)). This value is well supported by the theoretical curve for $\gamma l = 5.2$, but does not reach the maximum coupling transmission efficiency allowed by the crystal parameters (Fig. 6(a)). The maximum phase conjugate reflectivity given by theory for $\gamma l = 5.2$ is 125% at $q \sim 3.6$. The maximum value of phase conjugate reflectivity measured by us (121%) (Fig. 4(a)) is close to the maximum of this theoretical curve, where the reflectivity is very slowly changing with q (Fig. 6(b)).

Eq. (8) limits the operation range of our DPCM interconnection in the interval $0.14 < q < 7.1$ (for $\gamma l = 5.2$). In our experiment, the maximum value of q, which allowed the DPCM operation was obtained by extrapolation of the data at $\sim$8. Its minimum value was calculated with the Eq. (8), $q \sim 1/8$ (for $\gamma l = 5.2$).

The comparison of the experimental results with the simple analytical expressions for coupling transmission efficiency and phase conjugate reflectivity provided by the theoretical model of DPCM without absorption is useful for an evaluation of the efficiency and parameters of a DPCM interconnection device. Certainly, the absorption cannot be ignored in Rh:$BaTiO_3$ at 633 nm and the light induced transparency is present too, but theoretical modeling is more complicated when accounting for these processes and there are not yet analytical solutions for this general case.

On the other hand, the results for the coupling strength obtained in the frame of this simple model are consistent with that obtained in a two beam coupling experiment with the same crystal.

The mean value of the coupling coefficient γ, obtained in this experiment was $\gamma \sim 12\ \text{cm}^{-1}$. Taking into account that the upper limit of the interaction length inside the crystal in the two beam coupling experiment is equal to the crystal thickness (0.5 cm), the maximum value of the coupling strength can be $\gamma l \sim 6$. The comparison between DPCM coupling and the two beam coupling is a qualitative one, due to the different angles between the interacting beams involved in these nonlinear processes (the input beams and their own fanned beams in DPCM and the input beams in two beam coupling).

2.3. The coupling efficiency limits introduced by the intrinsic crystal losses

The upper limit of the coupling transmission efficiency in DPCM experiments depends on the total losses due to the absorption in the crystal and to the Fresnel reflections on the crystal faces. We have measured the reflection coefficients for the two angles of incidence, and the measured values, $R_\alpha = 1.28\%$ for $\alpha = 30°30'$ and $R_\beta = 12\%$ for $\beta = 60°30'$ are in good agreement with the theoretical values for these angles, 1.35% and 12.7%, respectively.

Taking into account the reflection losses A1 experiences at the crystal entrance face (R_α) and its diffracted component, A4, experiences at the crystal exit face (R_β), the total loss between the input and the output, including absorption in the crystal, is $(1 - R_\alpha)(1 - R_\beta)\exp(-\alpha l)$. In this case, the maximum crystal transmission can be 43%, which is smaller than the maximum coupling transmission efficiency experimentally measured (~50%). This fact can be explained by the light induced transparency in the crystal. As the change of the absorption coefficient was measured in the range 0.2–0.45 cm^{-1}, for crystals with similar doping concentrations, we can consider that the maximum coupling transmission efficiency experimentally measured is close to the maximum transmission allowed by the crystal.

2.4. Analysis of the competition of DPCM and SPPC for coupling optimization

In DPCM configuration, self-pumped phase conjugation (SPPC) can occur for each input beam when a part of their fanning reaches a crystal corner and totally reflects, forming an internal loop with a self-conjugation process. This is a parasitic effect for the DPCM bi-directional link due to the power loss outside of the interconnection, which decreases the coupling transmission efficiency.

The simple theoretical DPCM model previously described [7], leads to Eq. (5), which has nontrivial real solutions when $\gamma l > 4$. This limit sets the minimum DPCM threshold, for $q = 1$ [1,7]. On the other hand, the theoretical treatment of SPPC [21] leads to a coupling strength threshold for this process at $\gamma l = 4.68$ (in the loss-less case). Thus, the theoretical results show that normally DPCM is the winner in the competition with SPPC. However, an experimental check of the effect of SPPC on the DPCM efficiency and response time is necessary for the optimization of the DPCM link.

In our experimental DPCM interconnection, the SPPC process is more encouraged for the input beam A1, with smaller incidence angle with respect to the crystal c-axis. We have measured a maximum phase conjugate reflectivity of 16% for the mentioned incidence angle of A1 ($\alpha = 30°30'$), close to a crystal corner. In order to reduce this effect, we have displaced the incidence position of the beam A1 farther from the crystal corners, which was allowed by the crystal size.

In order to study the response time of this DPCM coupling, we have measured the dependence of the rising time of the conjugated beam in function of A2 beam power, in two situations: (a) both input beams (A1, A2) were switched on simultaneously, favoring the DPCM growing-up from the beginning; (b) the input beam A1 is switched on first, allowing SPPC to reach its maximum efficiency and, at this moment, the beam A2 is switched on, leading to the progressive decay of SPPC with simultaneous growth of the DPCM efficiency. From Fig. 7, one can remark that the DPCM rise time is lower in the case (a), but the differences between the two mentioned situations decrease with the A2 power increasing. We defined the DPCM response time by the time interval in which the phase conjugate power reached 90% of its saturation value, starting from its onset.

Experimentally, we have observed that, when A2 is too weak ($P_{A2} < 0.32$ mW, which means $q > 7.97$ for $P_{A1} = 2.55$ mW) the SPPC cannot be suppressed and the DPCM onset was not observed over long time. This observation is compatible with the range of operation provided by the experimental data from Fig. 6 and by the theoretical prediction (Eq. (8)), where the maximum value of q was found to be between 7 and 8.

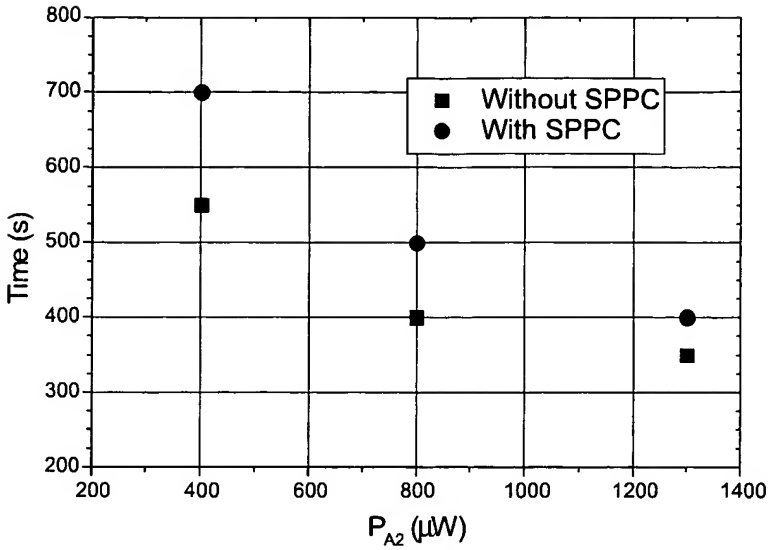

Fig. 7. The influence of the SPPC on the rising time (onset) of DPCM.

3. Analysis of the robustness of the DPCM interconnection against the beam direction changes

The DPCM configuration was efficiently used with incident beams in a considerable in-plane angular range (~10°) [2,12,13,15] around the angles from our experiment, as long as good overlapping and a low SPPC were ensured.

Considering DPCM interconnection of array sources, it is important to study the alignment requirements in the case of out-of-plane angular changes of one input beam with respect to the plane formed by the other one and the crystal c-axis (horizontal plane, H). We have rotated the beam A2 in the vertical plane, V, with the angle ϕ, preserving the incidence angles (α and β, respectively) of the beams in the plane (H). In Fig. 8, we show the coupling transmission efficiency and the phase conjugate reflectivity dependencies on the angle ϕ, for the beam power ratio $q = 1.9$, corresponding to the maximum of the coupling transmission efficiency. One can remark from Fig. 8

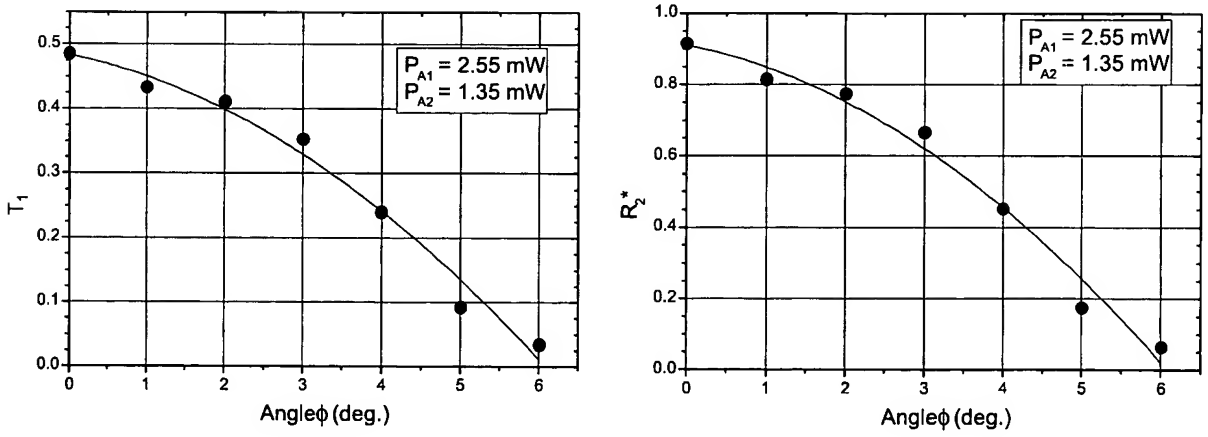

Fig. 8. The DPCM coupling efficiency versus the angle of A2 beam, ϕ, in the plane (V). The lines are eye guiding only.

that the coupling transmission efficiency and the phase conjugate reflectivity decrease in a similar manner with ϕ, becoming very small for $\phi > 6°$. Taking into account the positive and negative values of ϕ, our DPCM interconnection can operate efficiently in an angular range of $\sim 10°$ in the plane (V).

Consequently, we can conclude that this DPCM interconnection is robust against the incident beam angular misalignments. On the other hand, this property can be used for DPCM interconnection of modern array sources with large input angular range (e.g. centimeter sizes at locations of ~ 10 cm from photorefractive crystal).

4. The influence of laser beam modulation on the DPCM interconnection efficiency

The potential application of bi-directional interconnection using DPCM is to transfer signal information. This implies to modulate signals and to study the reciprocal influence of the input beam modulation and the adaptive interconnection. We have investigated this problem in two situations: (a) the unmodulated input beams were introduced together into the crystal to create an optimum interconnection channel and the modulation of one of the beams was switched on afterwards; (b) the modulated input beams were introduced together into the crystal to establish the interconnection channel.

In our experiment, we have modulated the stronger beam, A1, only, in order to compare the coupling transmission efficiency with the previous results in this paper. We have used for modulation a binary source (chopper) with the rate of 2 kbit/s and with the duty ratio of the light pulses of 0.5 (square wave). This binary source provides a strong modulation in which the crystal is half of the time illuminated with one beam only.

In Fig. 9(a), we show the results for the situation (a). One can observe that, when the modulation is switched on (at $t \sim 500$ s), the coupling efficiency does not change, indicating a stable and efficient interconnection channel. Once the interconnection channel is fully established, the modulation frequency of the input beam could be as high as possible, without optical limitations from the crystal parameters. Moreover, higher the modulation frequency smaller the channel change, due to large time constants of the crystal response, at these light power levels. In Fig. 9(b), a magnified view of the modulation switching from the graph of Fig. 9(a) is shown. The variable pulse frequency at the beginning of modulated signal corresponds to the transient onset of the mechanical chopper used as binary source in the experiment. In this figure, the modulation signal frequency seems to be different due to some missing points produced

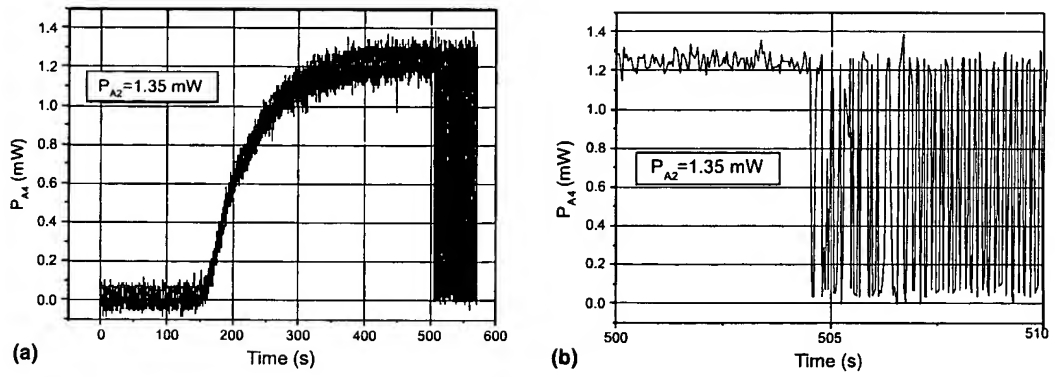

Fig. 9. (a) The influence of the input beam modulation on the coupling transmission efficiency, when the modulation of the input beam A1 was introduced after that the interconnection channel is established (after $\sim$ 500 s from the recording origin time); (b) a magnified view of the modulation switching from the graph of (a).

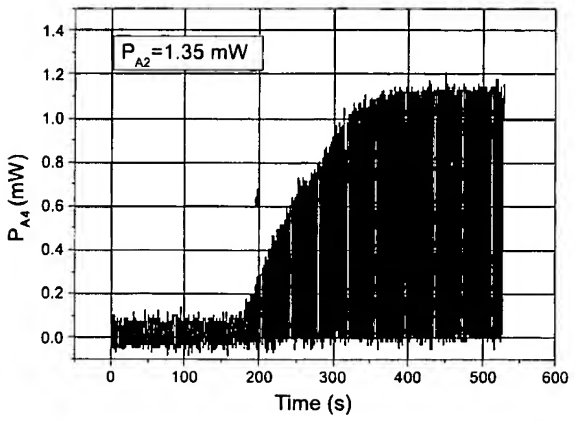

Fig. 10. The influence of the input beam modulation on the coupling transmission efficiency when the modulated input beam A1 were introduced into the crystal from the onset ($t = 100$ s) of the DPCM interconnection channel.

by the low sampling rate (25 samples/s) of the oscilloscope, at such long displaying times.

In Fig. 10, the result corresponding to the interconnection in situation (b) is shown, in which the modulation signal is present from the onset of the DPCM interconnection channel, $t = 100$ s. One can remark that the DPCM channel is developing in a similar manner with the situation (a), but with a slightly longer onset and rise time and with the slightly smaller final value of the coupling transmission efficiency.

In our experiment, the influence of the DPCM adaptive coupling on the input beam modulation was studied, too. With the same modulation source, the waveforms of modulated A1 input beam and of the output A4 beam were compared. Fig. 11 shows no observable changes induced by the DPCM channel on these waveforms.

5. Conclusions

A very efficient adaptive interconnection between two low power lasers, mutually incoherent, using a double phase-conjugate mirror in Rh:$BaTiO_3$ was demonstrated. Using low power incident beams, high phase conjugate reflectivity (~120%) and simultaneously, high coupling transmission efficiency (~50%) of the double phase conjugation process have been measured. Compared with analytical predictions of DPCM, these results are found in agreement. We have shown that the presence of self-pumped phase conjugation increases the build-up time of the DPCM interconnection channel. The robustness of the interconnection between the two lasers is demonstrated by acceptable coupling transmission efficiency for out-of-plane angular changes of the direction of one of the input beams in a range of ~10°. Binary laser beam modulation has shown no noticeable change of interconnection efficiency and reciprocally, the DPCM interconnection does not affect the transmitted information.

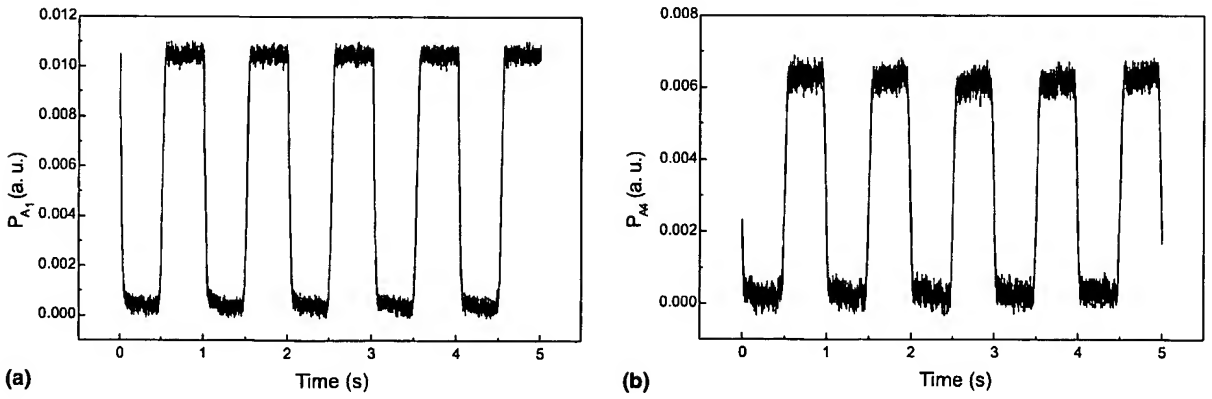

Fig. 11. The influence of the DPCM channel on the waveform of the modulation signal of A1: (a) the waveform of modulated A1 input beam; (b) the waveform of modulated A4 output beam.

Acknowledgements

A. Petris and V.I. Vlad gratefully acknowledge the support of the Royal Society and the Romanian Academy, in the frame of the Agreement of the Joint Scientific Research. Both thank Prof. J.C. Dainty for his continuous support and encouragement in this co-operation. They also acknowledge a grant of the Romanian Ministry of Education and Research.

References

[1] P. Yeh, Introduction to Photorefractive Nonlinear Optics, Wiley, New York, 1993.
[2] M. Snowbell, N. Strasman, B. Fischer, M. Cronin-Golomb, J. Lightwave Technol. 13 (1995) 55.
[3] S. Weiss, M. Segev, S. Sternklar, B. Fischer, Appl. Opt. 27 (1988) 3422.
[4] M.D. Ewbank, Opt. Lett. 13 (1988) 47.
[5] A.M.C. Smout, R.W. Eason, Opt. Lett. 12 (1987) 498.
[6] D. Wang, Z. Zhang, Y. Zhu, S. Zhang, P. Ye, Opt. Commun. 73 (1989) 495.
[7] S. Weiss, S. Sternklar, B. Fischer, Opt. Lett. 12 (1987) 114.
[8] B. Fischer, S. Sternklar, S. Weiss, IEEE J. Quantum Electron. QE-25 (1989) 550.
[9] Q.B. He, P. Yeh, C. Gu, R. Neurgaonkar, J. Opt. Soc. Am. B9 (1992) 114.
[10] P. Yeh, Appl. Optics 28 (1989) 1961.
[11] Qi-Chi He, IEEE J. Quantum Electron. QE-24 (1988) 2507.
[12] S.C. De La Cruz, S. MacCormack, J. Feinberg, Q. Byron He, H.K. Liu, P. Yeh, J. Opt. Soc. Am. B 12 (1995) 1363.
[13] M. Gruneisen, E. Seeberger, J. Milevski, K. Koch, Opt. Lett. 16 (1991) 596.
[14] Q.B. He, P. Yeh, Appl. Phys. B 60 (1995) 47.
[15] M. Kaczmarek, P. Hribek, R.W. Eason, Opt. Commun. 136 (1997) 277.
[16] L. Corner, R. Ramos-Garcia, A. Petris, M.J. Damzen, Opt. Commun. 143 (1997) 165.
[17] M. Cronin-Golomb, B. Fischer, J.O. White, A. Yariv, IEEE J. Quantum Electron. QE-20 (1984) 12.
[18] M.P. Petrov, S.L. Sochava, S.I. Stepanov, Opt. Lett. 14 (1989) 284.
[19] G. Martel, N. Wolffer, J.Y. Moisan, P. Gravey, Opt. Lett. 20 (1995) 937.
[20] S. MacCormack, J. Feinberg, M.H. Garrett, Opt. Lett. 19 (1994) 120.
[21] K.R. MacDonald, J. Feinberg, J. Opt. Soc. Am. 73 (1983) 548.

Appl. Phys. B 68, 1021–1025 (1999) / DOI 10.1007/s003409900008

Applied Physics B
Lasers
and Optics

Narrow bandwidth operation of high-power broad-area diode laser using cascaded phase-conjugate injection locking

H. Horiuchi[1], T. Shimura[1], T. Omatsu[2], O. Matoba[1], K. Kuroda[1]

[1] Institute of Industrial Science, University of Tokyo, 7-22-1, Roppongi, Minato-ku, Tokyo, 106-8558, Japan
(Fax: +81-3/3402-6375, E-mail: shimura@iis.u-tokyo.ac.jp)
[2] Faculty of Engineering, Chiba University, 1-33 Yayoi-cho, Inage-ku, Chiba, 263-8522, Japan

Received: 18 November 1998/Revised version: 29 January 1999/Published online: 7 April 1999

Abstract. A broad-area laser is injection-locked by another broad-area laser that is also injection-locked by a single-mode diode laser. Two double-phase conjugate mirrors of photorefractive $BaTaO_3$ are used to couple the master laser beams to the first slave laser, and the first slave laser output to the second slave laser. One of the double-phase conjugate mirrors is built up with the beams from two broad-area lasers. Two slave lasers are oscillating in single longitudinal mode at 808.5 nm and the spectral width is the same as that of the master laser. Final single-mode output power from the second slave broad-area laser is 840 mW, which is limited by the power of the injection beam. This work verifies the possibility of the multi-stage cascaded injection locking of high-power diode lasers with phase-conjugate injection.

PACS: 42.55.Px; 42.65.Hw

Output power of diode lasers is growing year by year. Now, several watts of output is available from a single-stripe broad-area laser, and the output power of the diode laser bars reaches several tens of watts. However, beam quality of these kinds of high-power diode lasers is quite poor. Transverse mode is far from TEM_{00}, and we cannot obtain large light intensity at a focused spot of the beam. Also, the oscillating spectrum is quite broad; typical spectral width is 2 nm for a broad-area laser. These drawbacks cause serious issues for actual applications such as, for example, laser isotope separation or gravitational wave detection by optical interferometers in which a really high-power and narrow spectral width tunable laser source is strongly needed.

One of the solutions of this problem is a system using an external cavity with a grating and/or phase-conjugate mirror. Some papers are presented and significant improvement of both spatial and temporal coherence of the high-power broad-stripe lasers [1] and laser diode arrays [2] are reported. In this system, the spectral width of the output beam is determined by the wavelength selectivity of the external cavity.

Another solution is the injection locking with a single-longitudinal and transverse-mode diode laser. We can obtain completely the same spectral line width as the master laser. Also, the transverse mode can be dramatically improved [3–5]. However, still we have some problems for injection locking of the high-power diode lasers. A broad-area laser has a quite thin and wide laser-active medium. Typical dimensions of the output facet are 1 μm × 100 μm. On the other hand, the output beam of the single-mode laser has a Gaussian profile. It is quite difficult to couple the laser beam of TEM_{00} mode to the thin and wide waveguide of the active medium. Of course, we can converge the TEM_{00} mode beam to the line-shaped output facet of the slave laser using cylindrical lenses and some other adjusting optics, but it is not so easy and coupling efficiency is not so high.

To overcome this difficulty, we can use a photorefractive mutual-pumped phase conjugator (MPPC) as a wave front converter. This technique is demonstrated for single-mode lasers [6, 7] and diode laser arrays [8]. We have shown that this technique is applicable to a broad-area laser using the photorefractive MPPC with the master single-mode laser and the broad-area slave laser [9]. Two input beams exchange their wave front through the MPPC, and the diffracted beam from the master laser becomes the phase conjugate wave of the direct output from the slave laser. Thus, the beam from the master laser propagates toward the slave laser and is coupled to the active medium automatically in accordance with the property of the phase conjugate wave. Coupling efficiency can be very high in this system because the injected beam is in the same transverse mode as the output beam. We have demonstrated the injection locking of the broad-area laser with photorefractive MPPC and achieved 550 mW output at single-longitudinal mode. The transverse mode was also improved. The M^2 value ranges from 61 without injection to 8 at the output power of 200 mW by injection locking. In this system, the maximum output power for single-longitudinal mode operation is limited by the power of injection beam. For the light injection power of 5 mW, the slave laser oscillates with multiple longitudinal modes when the output power exceeds 550 mW. To increase the final output power from the injection-locked laser, we have to increase the light injection power to the slave laser. Up to now, maximum output power of the commercially available single-mode diode laser is in the order of 100 mW. Thus, single-longitudinal mode output

power from the slave diode laser of this system is limited by the output power of the master laser.

In this paper, we present a cascade injection-locking system with MPPC to break these limitations. One broad-area diode laser is injection-locked by the single-mode diode laser. Then, the output beam of the locked slave laser, whose line width is completely the same as the master laser, is injected to the second broad-area laser. A key of this system is the building up of the MPPC with output beams from two broad-area lasers. We were successful and obtained fairly good diffraction efficiency. In principle, the number of laser chains of the cascading injection-locking system is unlimited and the final single-mode output power is determined by the output power of the laser at the final stage.

1 Experiments

The experimental setup is shown in Fig. 1. The first stage of the system is the same as our previous system [10]. A 1-W broad-area diode laser, LD1 (Sony SLD304XT) is injection-locked by the 50-mW single-mode diode laser LD2 (Sharp LT017MD). Both lasers are temperature-controlled and operating around 808.5 nm. The output beam of the master laser is incident on the nominally undoped $BaTiO_3$ crystal after passing through a collimator lens, and two 30-dB optical isolators. Incident power to the crystal is 20 mW. We drive the slave laser at 1.8 times the threshold current, and obtain output power of 400 mW. The beam of a broad-area laser has quite poor spatial coherence in the plane parallel to the hetero-junction because the active medium is very wide; the typical dimension is 200 μm. On the other hand, the spatial coherence in the plane perpendicular to the hetero-junction is rather high. The slave laser is placed in the plane of the hetero-junction vertical to the incident plane of the crystal to cause enough beam fanning to build up the double phase-conjugate mirror (DPCM). We use a half-wave plate to rotate the po-

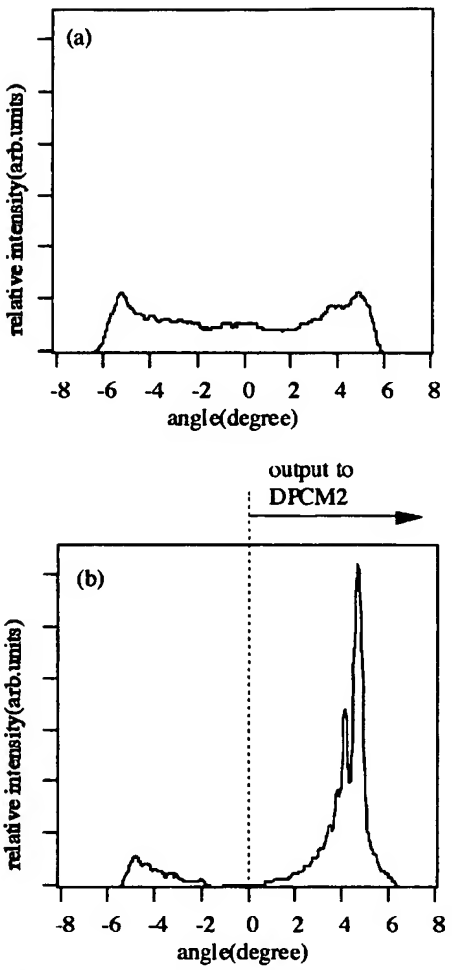

Fig. 2a,b. Far-field pattern of the LD2 for a free running, and b at injection locked. Half of the beam containing the main peak is led to the DPCM2

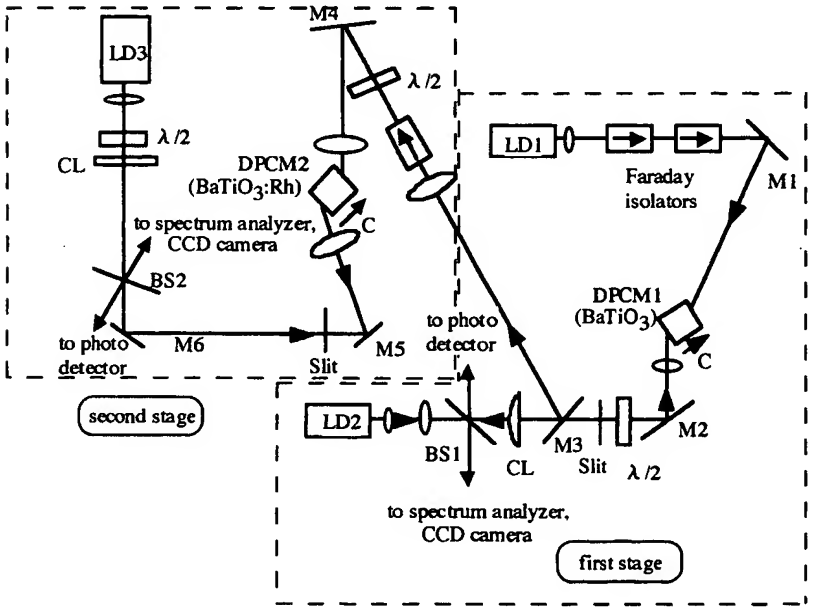

Fig. 1. Experimental setup of the two-stage cascade injection-locked system. LD1 is the single-mode master diode laser, LD2 and 3 are slave broad-area diode lasers which are placed with their hetero-junctions vertical to the plane. DPCM is a double phase-conjugate mirror, λ/2 is a half-wave plate, CL is a cylindrical lens, BS is a beam splitter, and M is a mirror. Slits, which select two or three transverse modes of the broad-area lasers, are placed in the horizontal plane. Mirror M3 bends the lower half of the output beam of the LD2 that contains the large main lobe. Upper half of the beam is going to the DPCM1

larization of the beam and make it an extraordinary ray to the crystal. Far-field pattern along the direction of the hetero-junction is made at a slit though the collimator and cylindrical lenses. The slit selects the vertical modes of the beam and only two or three modes are going to the DPCM1. Thus, the phase-conjugated injection beam couples to limited vertical modes of the slave laser and improves the far-field pattern of the slave laser.

When the slave laser is injection-locked, the far-field pattern of the beam of the slave laser has a large main peak and weak sub-peak as shown in Fig. 2. The angles of these two peaks from the optical axis of the laser are the same but at opposite sides. We pick up the half of the output beam containing the main peak by mirror M3. This half of the beam is fed to the DPCM2. The other half of the beam is going back to the DPCM1 through the slit.

The second stage of the system is basically the same as the first stage, except that the injection beam is coming from the injection-locked broad-area laser LD2. Another optical isolator is placed in the path from the LD2 to the DPCM2. The second slave laser LD3 is a 1.2-W broad-area laser (SDL, SDL2362-P2). It is also temperature-tuned and operating around 808.5 nm. We operated it at the injection current of 2.8 times the threshold current and obtained the output of 840 mW. We used Rh-doped $BaTiO_3$ as the DPCM2.

For both DPCM1 and 2, we set the return path optical length from the DPCMs to the slave lasers longer than the coherence length. This is to avoid making 2k gratings and reflection gratings [10, 11]. The DPCM with only transmission gratings shows high diffraction efficiency and good temporal stability [12].

2 Results and discussion

The procedure to build up the DPCM and injection locking at the first stage is the same as our single-stage system [9]. We achieve the single-longitudinal-mode operation of LD2. The oscillation line width is 80 MHz and the mode suppression ratio is 22 dB at the injection-locked operation.

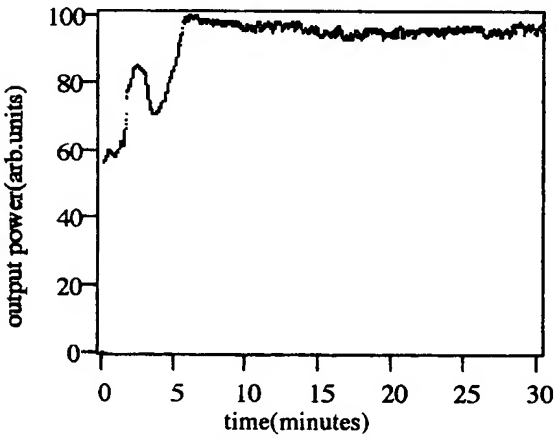

Fig. 3. Time evolution of the input power to the DPCM2. As LD2 is injection-locked, the main peak in the far-field pattern is growing, and the input to the DPCM2 is also growing

Then the main lobe of the output beam is going to the DPCM2 as a master beam to the LD3. Time evolution of the incident power to the second stage is shown in Fig. 3. We put the origin of the time at the moment that the outputs of LD1 and LD2 start to be incident to the DPCM1. At free running, half of the output power of the LD2 is incident at the second stage. According to the build-up of the DPCM1 and locking of LD2 by LD 1, the main lobe of the output beam of the LD2 is growing as shown in Fig. 2, and the power reaches a stable state after 7 min. The incident power to the second stage is about 80% of the total output power of LD2. At the same time, the spectrum of the LD2 changes from multi-mode oscillation to single-mode oscillation.

Then the DPCM2 is built up by the output beams from LD2 and LD3. In DPCM2, two beams are loosely focused and the beam diameters are 1–2 mm. The beam incident angles are almost the same as DPCM1, which is described in [9]. The DPCM2 is built up in several minutes and LD3 is injection-locked. Diffraction efficiency of the DPCM2 is 17% at stable state after the LD3 is injection-locked. It is a rather small value compared with that of DPCM1. For DPCM1, one of the incident beams is from the spatially single-mode laser and the other is from the broad-area laser. For DPCM2, both incident beams are from the broad-area lasers and the spatial coherence is not so high as single-mode lasers and the effective interaction length for the two-beam coupling is smaller.

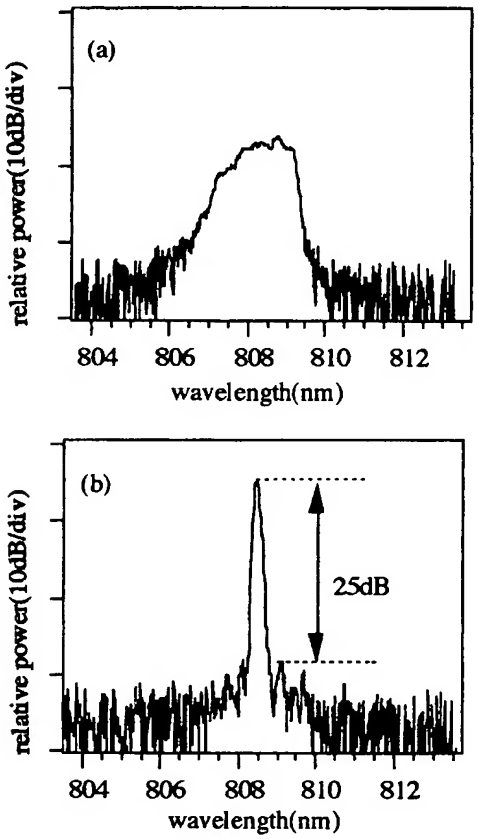

Fig. 4a,b. Oscillation spectrum of the second slave laser at output power of 840 mW, at a free running, and b injection-locked

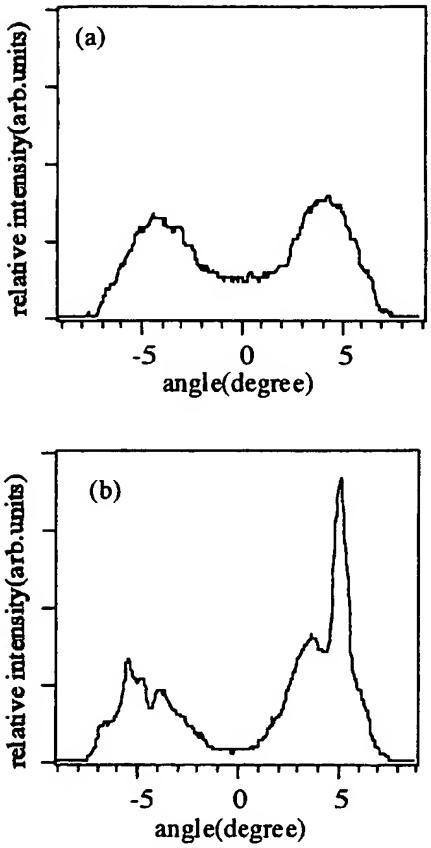

Fig. 5a,b. Far-field patterns of the second slave laser at output power of 840 mW, at a free running, and b injection-locked

This makes differences between the diffraction efficiencies of DPCM 1 and 2.

Once the DPCM2 is built up, LD3 is injection-locked by the output beam of LD2. Spectra of the output beam of LD3 with and without injection locking are shown in Fig. 4. They are measured by an optical spectrum analyzer (Anritsu, MS9001B1). At free running, the spectral width is about 2 nm in HMFW. Single-longitudinal-mode oscillation at 840 mW is achieved when LD3 is injection-locked. Mode suppression ratio is 25 dB. The locking state is sustained for several hours though the output power is not so stable as the output from the first stage.

Far-field patterns of the output beam of the LD3 with and without injection locking are shown in Fig. 5. The injection beam is coming to LD3 at the angle of $-5°$ and we can see a higher intensity peak at the opposite side. The qualitative change of the far-field pattern is the same as LD2. The right half of the far-field pattern of Fig. 5a contains 68% of the total power. Thus, improvement of the spatial coherence for LD3 is not so good as that for LD2 though we placed a narrow slit at the far-field position of the output beam of LD3, which is shown in Fig. 1. One possible reason for the imperfect far-field pattern is the difference of the structures of the active region of diode lasers. The LD2 has a simple single-stripe active region whose transverse dimensions are 200 μm × 0.05 μm. The structure of the LD3 is not fully open to view, but it may have some fine structure in its active region, whose emitting dimensions are 100 μm × 1 μm, to stabilize and limit the transverse mode. As seen in Fig. 2a and Fig. 4a, the output beam of the free-running LD3 has fewer transverse modes than that of LD2. It suggests that LD2 is more suitable for the improvement of the spatial mode by injection locking.

The power diagram of our whole system is shown in Fig. 6. As we can see, there is power loss at the second optical isolator OI2 and the DPCM2. It is due to the imperfect spatial beam quality of the output from LD2. Some amount of the light beam cannot go through the second optical isolator OI2, and the diffraction efficiency of the DPCM2 is not so high. These are the main factors of the power loss in the second stage of this system. Only 9.7 mW reaches the LD3 and the single-longitudinal-mode output power is limited to 840 mW. To increase the final output power, we should use an optical isolator with larger aperture. Another way to obtain

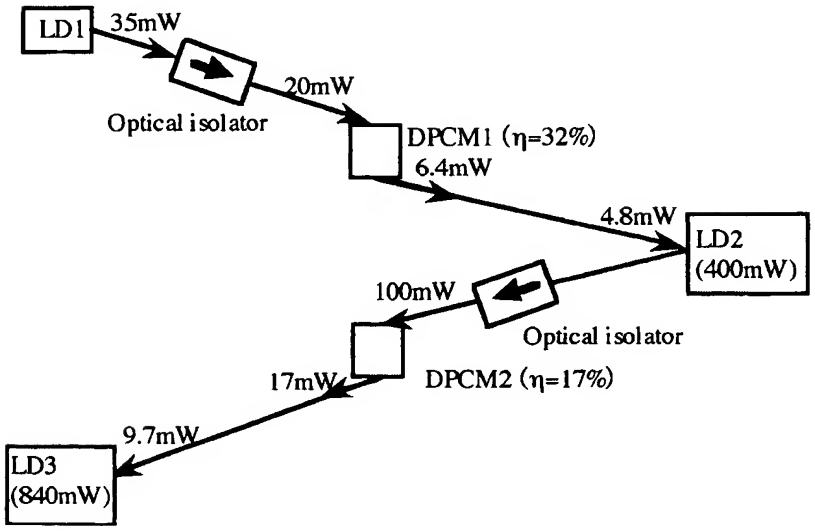

Fig. 6. Power diagram of the two-stage injection-locking system

higher total single-mode power is beam combining with the photorefractive two-wave mixing. We can combine the output beam from the LD2, which will not pass through the optical isolator, and the output from the LD3.

3 Conclusion

In summary, we achieved single-longitudinal mode operation of a broad-area laser with the output of 840 mW using two-stage phase-conjugate injection locking. We succeeded in the build-up of the photorefractive DPCM with two broad-area lasers. Spectral width of the final output beam is the same as that of the master oscillator. Spatial beam quality is improved though it is not perfect. In this work, we show that multi-stage cascaded injection-locking of broad-area lasers is possible with single-stripe broad-area diode lasers. We can expect that more single-mode power is obtained when we increase the number of cascades. In these systems, final power with single-longitudinal oscillation is determined by the output power of the broad-area laser in this system.

References

1. T. Omatsu, A. Katoh, K. Okada, S. Hatano, A. Hasegawa, M. Tateda, I. Ogura: Opt. Commun. **146**, 167 (1998)
2. M. Løbel, P.M. Petersen, P.M. Johansen: J. Opt. Soc. Am. B **15**, 2000 (1998)
3. G.L. Abbas, S. Yang, V.W.S. Chan, J.G. Fujimoto: Opt. Lett. **12**, 605 (1987)
4. L. Goldberg, M.K. Chun: Appl. Phys. Lett. **53**, 1900 (1988)
5. H. Tsuchida: Opt. Lett. **19**, 1741 (1994)
6. M. Segev, S. Weiss, B. Fischer: Appl. Phys. Lett. **50**, 1397 (1987)
7. T. Shimura, M. Tamura, K. Kuroda: Opt. Lett. **18**, 1645 (1993)
8. S. MacCormack, J. Feinberg, M.H. Garrett: Opt. Lett. **19**, 120 (1994)
9. K. Iida, H. Horiuchi, O. Matoba, T. Omatsu, T. Shimura, K. Kuroda: Opt. Commun. **146**, 6 (1998)
10. M.T. Gruneisen, E.D. Seeberger, J.F. Mileski, K. Koch: Opt. Lett. **16**, 596 (1991)
11. S.C. De La Cruz, S. MacCormack, J. Feinberg, Q.B. He, H.K. Liu, P. Yeh: J. Opt. Soc. Am. B **12**, 1363 (1995)
12. K. Iida, X. Tan, T. Shimura, K. Kuroda: Appl. Opt. **36**, 2491 (1997)

15 January 1998

ELSEVIER

Optics Communications 146 (1998) 6–10

OPTICS COMMUNICATIONS

Injection locking of a broad-area diode laser through a double phase-conjugate mirror

Kenichi Iida [a], Hisaki Horiuchi [a], Osamu Matoba [a], Takashige Omatsu [b], Tsutomu Shimura [a], Kazuo Kuroda [a,*]

[a] *Institute of Industrial Science, University of Tokyo, Roppongi, Minato-ku, Tokyo 106, Japan*
[b] *Department of Image Science, Chiba University, Yayoi-cho, Inage-ku, Chiba 263, Japan*

Received 6 May 1997; revised 28 August 1997; accepted 3 September 1997

Abstract

Injection locking of a 1-W broad-area diode laser was achieved using a double phase-conjugate mirror (DPCM). The DPCM was build up for the first time using the broad-area laser beam and it coupled an elliptical-shaped beam of a single-mode master laser efficiently into a broad-area laser's slit-shaped output facet. Single longitudinal mode operation up to 550 mW output was achieved by an injection beam power of no more than 0.6% of the whole output. The lateral beam pattern was also improved and the measured M^2 value of the locked beam greatly decreased compared with that of the free-running beam. $M^2 = 8$ for low-power operation and $M^2 = 28$ for high-power operation were achieved. © 1998 Elsevier Science B.V.

Keywords: Injection locking; Broad-area diode laser; Double phase-conjugate mirror

1. Introduction

The recent development of the thin-film crystal growth technique has enabled us to obtain a uniform and high-quality active gain layer for diode lasers, and broad-area lasers have now become a mainstream for obtaining a high-power laser beam, taking the place of phase-coupled diode arrays. Broad-area lasers have an advantage over phase-coupled arrays in that their structure is simple and the whole gain region can be efficiently used to produce a high-power beam. With a maximum output power of several watts, they are promising devices for high-power laser applications such as solid-state laser pumping, laser processing, and free-space optical communication. However, like phase-coupled arrays, the beam emitted from their widely spread active gain layer consists of multiple longitudinal and lateral modes, resulting in a poor temporal and spatial coherence. It is a serious issue to obtain high power density in both space and spectrum.

Injection locking is a technique that converts broad-area lasers into coherent and powerful light sources. A single-mode master laser beam is injected into the active gain region of broad-area lasers to force them to oscillate coherently with the master laser. The locked broad-area laser oscillates in a single longitudinal mode with an improved far-field emission pattern. Injection locking of broad-area lasers has been reported in a number of papers so far [1,2]. Just like the locking of arrays [3,4], a combination of cylindrical and spherical lenses is used to transform an elliptical-shaped single-mode master laser beam into a rectangular-shaped beam that is injected to the broad-area laser's tiny slit-shaped output facet. To obtain an optimized locking condition, however, strict adjustment in both the incident position and angle of the master laser beam is required. Furthermore, the preciseness of alignment determines the coupling efficiency of the injected beam into the slave laser cavity and, consequently, the

* Corresponding author. E-mail: kuroda@iis.u-tokyo.ac.jp.

PII S0030-4018(97)00518-X

maximum locked power attainable by finite power of the master laser beam.

Using a photorefractive mutually pumped phase-conjugate mirror (MPPCM), we can overcome these problems [5,6]. We use the MPPCM to guide the master laser beam into the active gain region of the slave laser. The MPPCM diffracts the master laser beam into a phase-conjugate replica of the slave laser output, which converges back along its path. As the master laser beam now has a beam profile that exactly matches the slave laser cavity, it is coupled with high efficiency without loss of energy. Moreover, at the speed of photorefractive response rate, the MPPCM compensates for any slight misalignment caused by frequency drift of the master laser beam or the change in external circumstances, and continues the efficient and stable beam injection into the slave laser cavity. Locking of a phase-coupled array laser using this technique was demonstrated in Ref. [7] and single-mode operation up to 450 mW was achieved. Here we describe injection locking of a broad-area laser using the double phase-conjugate mirror (DPCM) and analyse the results obtained.

2. Experiment

The top view of our experimental setup is shown in Fig. 1. The master laser is a 50-mW single-mode laser (Sharp LT017MD), whose wavelength is temperature-tuned to within the slave laser's 2-nm spectral width. After passing through a Faraday isolator and a $\lambda/2$ plate, its beam is incident on the nominally undoped $BaTiO_3$ crystal

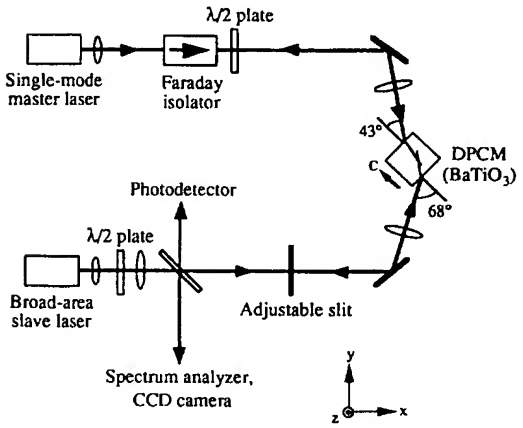

Fig. 1. Top view of experimental setup. A pair of extra-ordinary inputs from the master and slave lasers forms the DPCM in a $BaTiO_3$ crystal. The broad-area laser is set up with its lateral axes parallel to the z axis. The adjustable slit oriented along the y axis selects out a number of lateral modes from the laser far-field pattern distributed along the z direction as the DPCM input.

as an extra-ordinary beam with the power of approximately 10 mW. The external angle of incidence is 43° with respect to the crystal face normal.

The broad-area slave laser is a commercially available 1-W gain-guided laser (Sony SLD304XT) with a cavity length of 350 μm and an aperture width of 200 μm. We temperature-tune it and drive it at a current of 700 mA (equal to 1.4 times the threshold current) or 1040 mA (equal to 2.1 times the threshold current), where it produces an output power of 200 and 550 mW, respectively, at the wavelength of ~810 nm. When building the DPCM in a $BaTiO_3$ crystal, not only the polarization but also the spatial coherence of inputs is required in the direction within the crystal extraordinary (a–c) plane. The spatial coherence of the beam from the broad-area laser is deteriorated along its lateral axis, which is in the junction plane and perpendicular to the optical axis, but the spatial coherence is rather preserved along its transverse axis, which is perpendicular to the junction plane. Therefore, we set up the laser with its lateral axis parallel to the z axis in Fig. 1. With the help of an additional half-wave plate, we can supply the crystal with a beam whose polarization and better spatial coherence both lie in its extraordinary plane. Here a combination of a high-NA plastic lens and a spherical lens placed in front of the laser generates a twin-lobed lateral far-field pattern of the broad-area laser with a width of ~3 mm in the z direction. An adjustable slit oriented along the y axis is then used to perform its spatial filtering similar to the one reported in Ref. [7]. The slit width is approximately 0.25 mm. We adjust the position of the slit onto one of the peaks of the twin lobes and extract some of the dominant broad-area lateral modes [8] of the free-running laser for the DPCM input. The initial DPCM input power is approximately 10 mW for the broad-area laser's 200-mW operation and approximately 25 mW for the 550-mW operation. However, it is reduced after locking is achieved due to the change of the far-field pattern of the broad-area laser. The external angle of incident beam is 68° with respect to the crystal face normal.

With this experimental setup, we succeeded to build up the DPCM for the first time using the broad-area laser beam and diffraction efficiency of more than 50% was attained. The DPCM was the only MPPCM configuration we could build up with our crystal. In this experiment, 53% of the DPCM output reaches the slave laser constantly and is efficiently coupled into its cavity to bring about the locking. The beam sampler placed in the path of the slave laser beam picks off a small portion of the phase-conjugate beam directed by the DPCM to the broad-area laser, whose power is measured by a photodetector. It also samples out the slave laser output for spectrum and beam pattern measurements. The spectrum is measured by an optical spectrum analyzer (Anritsu MS9001B1) with a resolution of 0.1 nm, and by the scanning Fabry-Perot etalon (Coherent 240-1C) with a

resolution of 35 MHz. The near-field and far-field beam patterns are observed by a CCD camera.

3. Results and discussion

After a minute of formation time of the DPCM, it starts to direct the master laser beam into the broad-area laser facet as a phase-conjugate beam of its own output to bring about the locking. Fig. 2 shows the output spectrum of the (a) free-running and (b) injection-locked broad-area laser obtained by the spectrum analyzer. At free-running, the broad-area laser oscillates in multilongitudinal modes with a FWHM of 2 nm. As the DPCM grows up and the injected beam power increases, the broad-area laser gradually switches to the oscillation in the master laser mode. When the injected beam power finally reaches a threshold power for complete locking, the laser starts to oscillate in a single longitudinal mode. Its side-mode suppression ratio is 24 dB, and a linewidth of 80 MHz is measured by the scanning Fabry-Perot etalon as shown in Fig. 3. These values are approximately the same as those of the master laser. The threshold power in our experiment is 0.6% of the whole laser output, and above this injection level no change in the spectrum or beam patterns is observed. It should be noted, however, that stronger injection beam power provides stable locking with a broader locking bandwidth. Overlapping both the master and slave laser beams on the CCD camera produces stable interference fringes of high visibility, from which we evaluate the degree of coherence [9] of ~ 0.8 between the two lasers. This proves the coherent oscillation and the stable phase-locking of the two lasers.

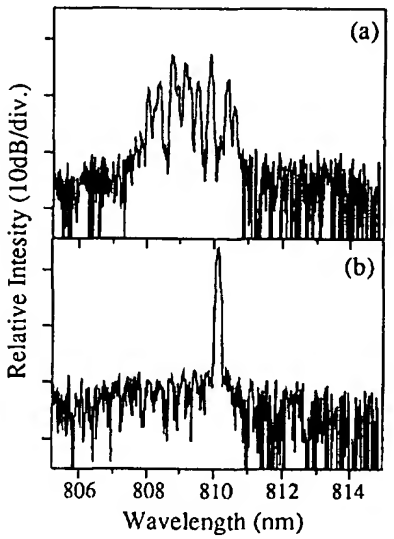

Fig. 2. The spectra of (a) a free-running and (b) a locked broad-area laser measured with an optical spectrum analyzer.

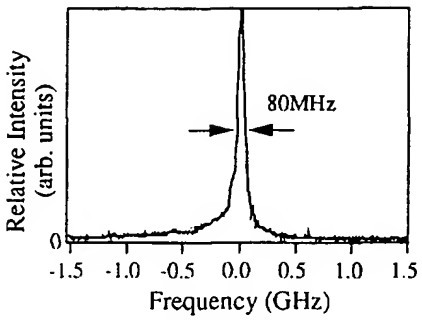

Fig. 3. The spectrum of a locked broad-area laser measured with a scanning Fabry-Perot etalon.

Here we should mention that the DPCM works better with mutually incoherent inputs and, as the coherence increases, its reflectivity decreases and fluctuates due to the presence of the reflection and 2-k gratings [10,11]. In our setup, however, as we took the distance between the slave laser and the DPCM longer than the master laser's 4-m coherence length, two DPCM inputs are kept mutually incoherent even after locking is achieved. The DPCM with only the transmission gratings shows high diffraction efficiency with a good temporal stability and is able to retain stable locking for many hours [12].

Far-field and near-field patterns of the locked and the free-running slave laser are observed by the CCD camera. By narrowing the width of the slit in the far-field to approximately 3 times the 0.20° diffraction limit of the laser's 200-μm-wide aperture, we can optimize the far-field pattern of the locked slave laser. Fig. 4 shows the far-field and near-field patterns of the broad-area laser operated at the output of 200 mW. At free-running, incoherent superposition of multiple broad-area modes produces the twin-lobed far-field pattern (Fig. 4a) and the top-hat near-field distribution (Fig. 4b).

Preserving the total power, these patterns change drastically by injection locking. The master laser beam directed by the DPCM to the slave laser has the same spatial and phase profile as the preferred modes of the free-running laser selected by the slit. It excites modes of the same orders in the cavity, and their resonant amplification produces a combination of a strong main lobe and a weak sub lobe in the far-field (Fig. 4c) and a large filamentation in the near-field (Fig. 4d). From the emission angle of two lobes and the number of stripes, we can understand that the coherent superposition of $m = 29$ and $m = 30$ modes driven in phase with the master laser at the same frequency is a dominant factor for constructing these beam patterns.

The main lobe beam, which appears at an angle equal to but opposite to that of the injected beam, contains 80% of the whole output and its divergence is narrowed to 0.38°, or 1.9 times the 0.20° diffraction limit. Let the main lobe contain all the beam with the positive emission angle and we obtain the Strehl ratio of 0.33. The Strehl ratio is

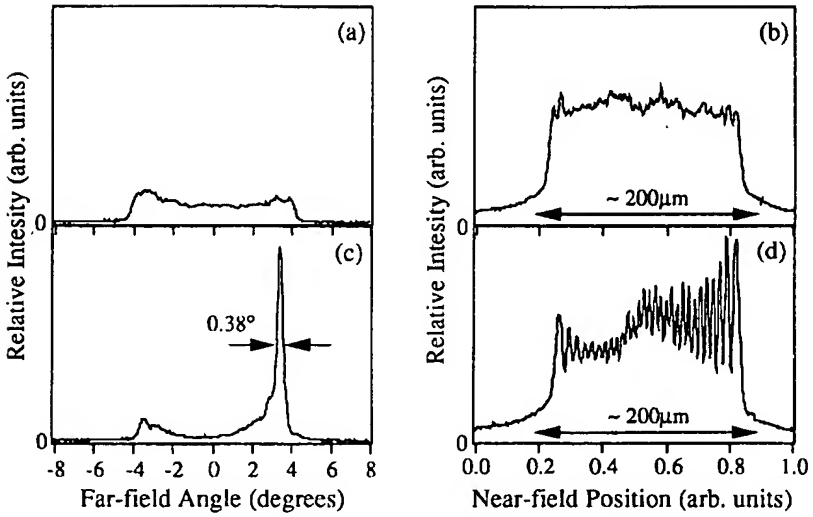

Fig. 4. Far-field and near-field patterns of a broad-area diode laser operated at the output of 200 mW: (a) and (b) at free-running, (c) and (d) at locked state.

determined as the ratio of the peak power density of the main lobe to that of the diffraction pattern formed by the plane wave coming out from the 200-μm-wide aperture having the same total power. The main lobe beam can be collected as the useful output of the system by placing a scraper mirror just at the slit. It is fortunate that in the direction to the DPCM the sub lobe still remains in our locking scheme. This lobe is not a free-running component but is also a locked remaining component, which we can confirm from its coherence as high as 0.8 between the master laser beam. It continues to pass through the slit to serve as an input for the DPCM and guides the master laser beam into its cavity to preserve locking for many hours.

Similar results are obtained when the slave laser is driven at 550 mW output (Fig. 5). A combination of the lateral modes $m = 37$ and $m = 38$ produces the asymmetric far-field pattern (Fig. 5c) along with the modulation in the near-field (Fig. 5d). However, the lateral mode selectivity seems to be somewhat degraded during this experiment, resulting in involvement of some other adjacent modes. Consequently, broadening and splitting in the far-field lobe (Strehl ratio of 0.17) and decrease in the near-field modulation can be noticed.

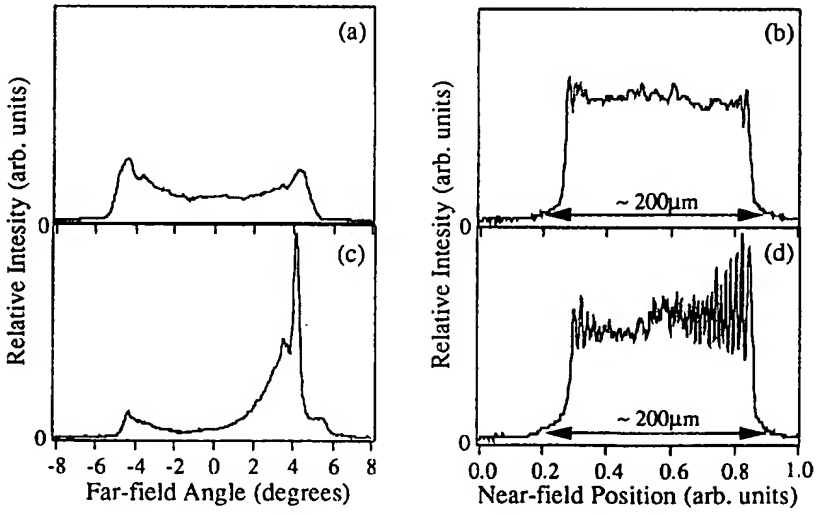

Fig. 5. Far-field and near-field patterns of a broad-area diode laser operated at the output of 550 mW: (a) and (b) at free-running, (c) and (d) at locked state.

Table 1
M^2 values (in the lateral direction along the junction plane) of the free-running and locked broad-area laser

Slave laser output	Free-running	Locked
200 mW	$M^2 = 61$	$M^2 = 8$
550 mW	$M^2 = 86$	$M^2 = 28$

Note that the values for the locked case represent only the main lobe beam, while those for the free-running case represent the whole output beam.

The locking achieved in our experiment is very stable. While the temporal fluctuation of the DPCM output is ~ 10%, the main lobe power of the locked slave laser shows high stability with fluctuation of less than 1%. As it is the main lobe beam that can be extracted as a coherent output from the system in our locking scheme, we measured its effective M^2 value (in the lateral direction along the gain layer plane) to evaluate its beam quality. We take out the main lobe beam and pass it through a cylindrical lens to produce the beam waist region which we can scan by a CCD camera. The beam spot size in each scanned plane is obtained by employing the second moment determination method [13], whose variation is curve-fitted to determine the M^2 value. Table 1 shows the comparison between the M^2 values in the free-running and locked cases when the broad-area laser is operated at the output of 200 and 550 mW. Note that the M^2 values for the locked case only represent the main lobe beam, while that for the free-running case represents the whole output beam. Under only 20% energy loss in the sub lobe, injection locking greatly reduces the M^2 values of the broad-area laser and enhances its collector efficiencies.

In our experiment, an injected beam power of only 0.6% of the whole broad-area laser output is enough to achieve complete locking. This value seems to be less than half of the power required in the conventional locking reported in Ref. [2]. The use of the DPCM enables us to double the coupling efficiency of the master laser beam into the slave laser cavity with significantly simplified optic alignment. Meanwhile the locked far-field pattern obtained in our experiment has still a wider divergence angle than the one obtained in Ref. [2], which was 1.3 times the diffraction limit. In our locking scheme, it is the width of the slit placed in the far-field that determines the degree of lateral mode selectivity and, by narrowing the slit width, the divergence angle of the main lobe can be smaller. However, if we make the slit width too narrow, the DPCM input power from the slave laser decreases, which directly leads to reduction of the diffraction efficiency of DPCM, and enough injection beam power to lock the slave laser will become unattainable.

This problem can be solved by building up a better MPPCM using a better crystal such as a rhodium-doped $BaTiO_3$ crystal, which has enhanced photorefractive sensitivity at near-infrared wavelengths. The MPPCM of better phase-conjugate fidelity or higher diffraction efficiency can produce phase-conjugate beams of more power with inputs of small power. This allows us to narrow the slit width still more at the cost of the MPPCM input power from the slave laser to enhance lateral mode selectivity, while obtaining enough injection beam power into the slave laser to achieve complete locking.

4. Conclusions

In summary, we have demonstrated an efficient and alignment-free injection locking of a broad-area diode laser using a DPCM. The DPCM was build up for the first time using the broad-area laser beam and it coupled a single-mode master laser beam efficiently into the laser gain region. The broad-area laser was forced to oscillate with exactly the same frequency as the master laser and a single longitudinal mode output up to 550 mW was achieved by an injection beam power of only 0.6% of the whole output. Improvement in that lateral mode structure was also achieved and we saw the M^2 value of the locked beam greatly reduced compared with that of the free-running case.

Acknowledgements

We are grateful to Michio Oka at SONY Research Center for supplying the broad-area diode lasers.

References

[1] G.L. Abbas, S. Yang, V.W.S. Chan, J.G. Fujimoto, Optics Lett. 12 (1987) 605.
[2] L. Goldberg, M.K. Chun, Appl. Phys. Lett. 53 (1988) 1900.
[3] L. Goldberg, H.F. Taylor, J.F. Weller, Appl. Phys. Lett. 46 (1985) 236.
[4] J.-M. Verdiell, R. Frey, J.P. Huignard, IEEE J. Quantum Electron. 27 (1991) 396.
[5] M. Segev, S. Weiss, B. Fischer, Appl. Phys. Lett. 50 (1987) 1397.
[6] T. Shimura, M. Tamura, K. Kuroda, Optics Lett. 18 (1993) 1645.
[7] S. MacCormack, J. Feinberg, M.H. Garrett, Optics Lett. 19 (1994) 120.
[8] J.-M. Verdiell, R. Frey, IEEE J. Quantum Electron. 26 (1990) 270.
[9] M. Born, E. Wolf, Principles of Optics, Pergamon, Oxford, 1970, p. 501.
[10] M.T. Gruneisen, E.D. Seeberger, J.F. Mileski, K. Koch, Optics Lett. 16 (1991) 596.
[11] S.C. De La Cruz, S. MacCormack, J. Feinberg, Q.B. He, H.K. Liu, P. Yeh, J. Opt. Soc. Am. B 12 (1995) 1363.
[12] K. Iida, X. Tan, T. Shimura, K. Kuroda, Appl. Optics 36 (1997) 2491.
[13] A.E. Siegman, Proc. SPIE 1868 (1993) 2.

Injection locking a laser-diode array with a phase-conjugate beam

Stuart MacCormack and Jack Feinberg

Departments of Physics and Electrical Engineering, University of Southern California, Los Angeles, California 90089-0484

M. H. Garrett

Centre de Recherche en Optoélectroniques, Sandoz-Huningue S.A., Avenue de Bâle, Huningue 68330, France

Received July 16, 1993

We use a mutually pumped phase conjugator to guide the output beam of a single-mode laser diode into the active region of a high-power laser-diode array. This injected beam locks the frequency of the array, causing it to emit a single, 1.45 times diffraction-limited, continuous-wave output beam containing 85% of the array's total output power. Phase-conjugate injection dramatically improves the coupling into the laser array, so that less than a milliwatt of injected power is sufficient to lock all the array's 450-mW output to the frequency of the master laser.

Injecting light from a single-mode laser into a laser-diode array can narrow the array's output spectrum and produce a nearly diffraction-limited output beam.[1] Over a narrow range of wavelengths and injection angles, the laser array becomes a slave to the master laser's injecting beam; it simply becomes a waveguide with optical gain and amplifies the injected beam at the expense of the array's own free-running modes. However, this occurs only if the master laser beam's frequency, position, and incident angle are just right,[2] and these constraints place great demands on the master laser beam's frequency stability, shape, and alignment. Here we demonstrate an injection-locking scheme that overcomes these problems: we use a mutually pumped phase conjugator to aim the master laser beam precisely into the gain region of the laser array.

A mutually pumped phase conjugator couples two optical beams and directs each beam down the throat of the other.[3,4] The two incident light beams typically have slightly different frequencies and so are not coherent with each other. The conjugator transfers spatial and phase information from one beam to the other, so that the two beams leave the device as phase-conjugate replicas of each another. We use a photorefractive crystal of barium titanate as our mutually pumped phase conjugator. The ~1-s response time of this conjugator automatically adjusts to gradual changes in either the position or the angle of incidence of the two input beams. Using a mutually pumped phase conjugator to direct the laser beams eases the problem of beam alignment and shape by a factor of ~1000, from one of micrometers and millidegrees into one of millimeters and degrees.

Figure 1 shows our experimental setup. The slave laser is an off-the-shelf, 1-W laser-diode array (SDL 2462-P1) mounted on a temperature-controlled heat sink and operated at a wavelength of ~800 nm. We conservatively operate the laser at a current of 1.0 A (equal to 2.1 times the threshold current), where it produces a continuous-wave, free-running output power of 450 mW. (We operate the laser below its maximum rated output power to suppress oscillation on its free-running modes. Alternatively, we could reduce the slave laser's output coupler reflectivity and thereby increase the self-oscillation threshold.) A high-numerical-aperture lens collects the horizontally polarized output beam and directs it toward a cylindrical and spherical lens pair. This lens combination generates a pseudo twin-lobed far-field pattern with a width of ~10 mm. One lobe is incident upon an adjustable slit placed in the far field. Light transmitted through the slit is weakly focused by a spherical lens into an approximately 1 mm × 1 mm spot on one a face of the $BaTiO_3$ crystal. Its external angle of incidence is 65° to the crystal face normal. Our blue-colored $BaTiO_3$ crystal (named Bleu) measures 6.1 mm × 6.6 mm × 5.9 mm and is mounted with its c axis in the vertical plane. (Blue $BaTiO_3$ has an enhanced photorefractive response at near-infrared wavelengths compared with the usual pale-

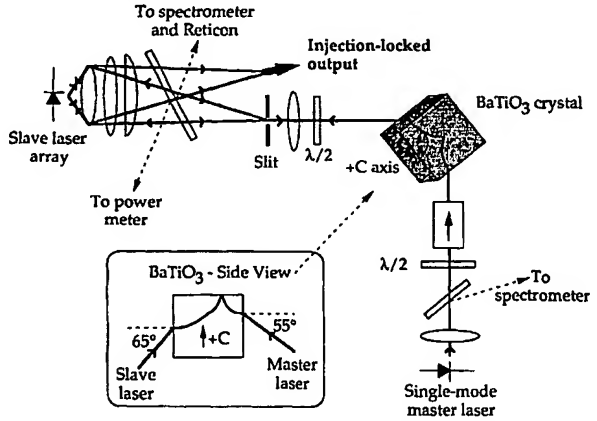

Fig. 1. Experimental setup. The combination of a Faraday polarizer and a $\lambda/2$ plate isolates the single-mode master laser. The slit selects one lobe of the array slave laser. Both the master and slave laser beams enter the $BaTiO_3$ crystal and fan toward its top face. (The crystal's $+c$ axis faces up, normal to the plane of this figure.) The inset shows a side view of the $BaTiO_3$ crystal and the bird-wing pattern made by the laser beams.

0146-9592/94/020120-03$6.00/0

yellow $BaTiO_3$.[5]) We use a half-wave plate to make the array's output polarization parallel to its direction of spatial coherence, which is perpendicular to the plane of the laser gain region.[6,7]

The master laser is a 100-mW, temperature-tuned, single-mode laser (SDL 5412-H1). We temperature tune this master laser's frequency to lie anywhere within the slave laser's 2-nm-wide, free-running output spectrum. Its polarized output is collected by a high-numerical-aperture lens and directed through a half-wave plate and a Faraday isolator to make it an extraordinary ray at the barium titanate crystal. (The Faraday isolator prevents light from the slave laser from feeding back into the master laser and causing frequency instabilities. Good optical isolation is especially important here since a fraction of the array's output is converted into the phase-conjugate replica of the master laser's beam.) We direct ~8 mW of output from the master laser into the $BaTiO_3$ crystal face opposite the a face entered by the slave laser and positioned closer to the crystal's positive c face than to the slave laser's input beam. This injected beam makes an external angle of 55° to the crystal face normal. We use asymmetric beam positions because the narrow-frequency, master laser beam fans more strongly in the crystal than does the broad-bandwidth, slave laser beam. We perform beam power, frequency, and shape measurements on reflections from optical flats placed in the paths of the master and slave laser beams. We analyze the optical beams' frequencies with a Spex 0.75-m double-grating spectrometer and a Newport SR-200 spectrum analyzer (finesse >10,000). We monitor the beams' shapes with a 512-element scanning linear photodiode array placed in the far field.

Within a few seconds after the master and the slave laser beams illuminate the crystal, the beams bend and join to form an asymmetric bird-wing mutually pumped phase conjugator.[4] The conjugator directs the master laser beam into the phase-conjugate replica of the slave laser beam. This injected beam now has the same spatial and phase profile as one of the preferred transverse array modes of the free-running array and so has the optimum angle and profile for injection locking the array.[8] Once the array is injection locked, the array switches to emit predominantly a single lobe that appears at an angle equal to but opposite that of the injected beam.

As shown in Fig. 2, this strong output lobe is accompanied by a weaker secondary lobe that continues to illuminate the bird-wing conjugator. These two lobes compete and reach a stable steady state. For example, if the power directed into the conjugator decreases as a result of greater locking efficiency, then the conjugator becomes less efficient. This decreases the power injected into the array, which in turn decreases the power directed into the output lobe, thereby restoring the equilibrium. We found that directing too much master laser power (>30 mW) into the conjugator can make the injection locking too efficient, so that all the array's output suddenly switches into the output lobe at he expense of the secondary lobe. With no light now coming from the array to the conjugator, the conjugator turns off, and locking ceases.

Once the array is injection locked, the angular width of the output lobe changes according to the width of the far-field aperture. We adjust this aperture to optimize the power in the array's output lobe while still keeping its divergence near the 0.29° diffraction limit of the array's 200-μm-wide emitting region. For example, with the adjustable aperture set to produce an output beam divergence of 1.5 times the diffraction limit, the output beam has an elliptical Gaussian profile and contains 85% of the array's total output (384 mW). The remaining output power is in the secondary lobe, with practically no emission outside these two locked lobes. When the array is locked, the angular position of the main lobe remains constant, even with small perturbations to the far-field aperture width, ambient temperature, or position of the master laser beam. The stability of the locked far-field lobe intensity is good. Over periods of hours, we measure peak-to-peak fluctuations of less than 10% in the main lobe intensity. These intensity fluctuations arise predominantly from the 20% fluctuations in the conjugator's transmissivity. We observe no steering of the far-field lobe with small changes in the master laser's drive current.

The free-running array lases on many longitudinal modes simultaneously. However, the injection-locked array operates only at the master laser's single wavelength. (Frequency pulling and changes in the far-field profile were previously observed for two arrays coupled by a mutually pumped phase conjugator.[9]) No other output frequencies are present to within the 20-dB sensitivity of our spectrometer. Figure 3 shows that the bandwidths of the master and slave laser outputs are identical to within the 750-MHz resolution of our spectrum analyzer. Overlapping the master and slave laser outputs on a CCD camera produces stable high-visibility interference fringes, implying that the two lasers are locked and coherent with each other. (We have shown previously that the bird-wing conjugator performs well even with mutually coherent input beams.[10]) In our experiments, we

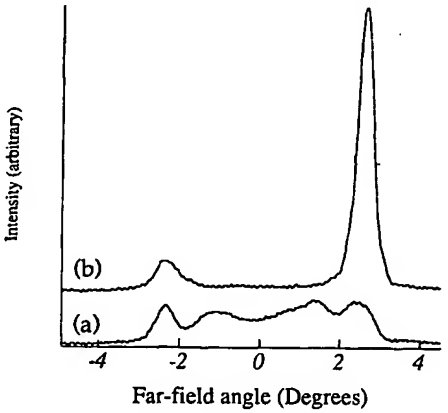

Fig. 2. Far-field spatial pattern of the diode array (a) when free running and (b) when injection locked. The FWHM of the main lobe in (b) is 0.38°, which is 1.45 times the diffraction limit (a Strehl ratio of 0.37). The total output power for each case is 450 mW.

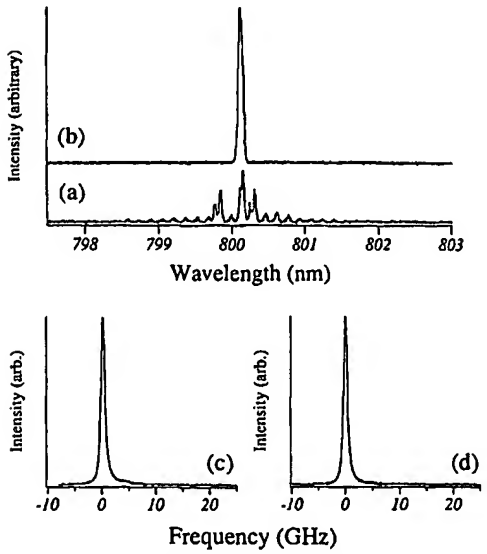

Fig. 3. Diode-array spectra measured with a 1.4-m spectrometer when (a) free running and (b) locked. Once the array is locked, (c) and (d) show the high-resolution spectra of the slave and master laser output beams, respectively; their frequency bandwidth is narrower than the 750-MHz resolution of our spectrum analyzer.

observe no contribution to the light injected into the array from any backscattering gratings in the $BaTiO_3$ crystal.

Consider the injection-locking process as the amplification of a signal beam in a Fabry–Perot amplifier.[11] We can then judge the effectiveness of different geometries by comparing the values of their small-signal gain, G, defined as the ratio of the power contained in the locked lobe to the injected power, for operation in the unsaturated regime. For conventional injection-locking geometries, G typically ranges from 19 to 23 dB.[12,13] However, we are not operating in the unsaturated regime. As discussed above, increasing the power incident upon the crystal from the master laser does not necessarily increase the power injected into the array. Nevertheless, even when operating in a saturated regime, we obtain a locked output of >380 mW for an injected signal of 0.50 mW, corresponding to a saturated gain of 29 dB. Below this injection level the spatial shape of the output lobe deteriorates.

In our experiments the small-signal gain G is large because our injected signal is the phase-conjugate replica of one of the natural modes of the slave laser array. Consequently, it is efficiently coupled into the slave laser waveguide and has an ideal overlap with the gain profile of the laser. This leads to efficient gain extraction and to saturation of the amplification even with small injected power. If we permit a somewhat degraded output beam shape and compute the locking efficiency using the total output power of the slave array (i.e., both the output and the secondary lobes), then we can boast of a frequency-locked output of 450 mW for an injected power of 0.27 mW, which corresponds to a gain of 32 dB.

At steady state our bird-wing conjugator typically transforms ~5% of each incident beam into a phase-conjugator replica of the other beam. For example, in the setup shown in Fig. 1 the power from the master laser incident upon the $BaTiO_3$ crystal was 8.2 mW, while the power deflected by the conjugator toward the slave laser was 0.50 mW, which gives a phase-conjugate transmission of 6%. A transmissivity as large as 35% has been observed for mutually pumped phase conjugators in the near infrared,[14] but we were unable to achieve such large values in our experiments.

We have shown that a phase-conjugate injection beam significantly improves the ease of alignment and the efficiency of locking a laser-diode array. The ability of a small injected power to lock a laser array becomes important for locking higher-power laser diodes or locking multiple laser arrays. In these cases, the success of injection locking will depend on the power available from the single-mode master laser. With conventional injection locking the currently available 100-mW single-mode lasers could lock a maximum of ~10 W of slave laser output. However, with phase-conjugate injection locking the same 100-mW laser has the potential for locking slave laser arrays of as much as 100 W.

We gratefully acknowledge support by grant F49620-92-J-0022 from the U.S. Air Force Office of Scientific Research.

References

1. L. Goldberg and J. F. Weller, Appl. Phys. Lett. **46,** 236 (1985).
2. M. K. Chun, L. Goldberg, and J. F. Weller, Opt. Lett. **14,** 272 (1989).
3. B. Fischer and S. Sternklar, Appl. Phys. Lett. **51,** 74 (1987).
4. M. D. Ewbank, Opt. Lett. **13,** 47 (1988).
5. G. W. Ross, P. Hribek, R. W. Eason, M. H. Garrett, and D. Rytz, in *Conference on Lasers and Electro-Optics,* Vol. 11 of 1993 OSA Technical Digest Series (Optical Society of America, Washington, D.C., 1993), paper CFC4.
6. S. MacCormack and J. Feinberg, Opt. Lett. **18,** 211 (1993).
7. M. Cronin-Golomb, Tufts University, Medford, Mass. 02155 (personal communication, 1991).
8. H. Adachihara, O. Hess, R. Indik, and J. V. Moloney, J. Opt. Soc. Am. B **10,** 496 (1993).
9. M. Segev, S. Weiss, and B. Fischer, Appl. Phys. Lett. **50,** 1397 (1987).
10. S. C. De La Cruz, S. MacCormack, and J. Feinberg, in *Conference on Lasers and Electro-Optics,* Vol. 11 of 1993 OSA Technical Digest Series (Optical Society of America, Washington, D.C., 1993), paper CThS54.
11. G. L. Abbas, S. Yang, V. W. S. Chan, and J. G. Fujimoto, Opt. Lett. **12,** 605 (1987).
12. L. Goldberg and J. F. Weller, Appl. Phys. Lett. **53,** 1900 (1988).
13. L. Goldberg and J. F. Weller, Electron. Lett. **22,** 858 (1986).
14. G. W. Ross and R. W. Eason, Opt. Lett. **18,** 571 (1993).